Vectored Transmission for Digital Subscriber Line Systems

George Ginis, *Student Member, IEEE* and John M. Cioffi, *Fellow, IEEE*

***Abstract*—This paper describes the "vectored" transmission technique for digital subscriber line (DSL) systems, which utilizes user coordination at the central office or optical network unit. This method exploits the colocation of the downstream transmitters and of the upstream receivers, in order to achieve far-end crosstalk (FEXT) cancellation and perform multiuser transmission optimization. The performance improvements are particularly pronounced in environments with strong FEXT such as in very high-speed DSL.**

Discrete multitone is employed for each user with additional constraints on the cyclic prefix length and with the assumption of block-synchronized transmission and reception for downstream and upstream transmission correspondingly. Within each tone, upstream crosstalk is removed by multiple-input–multiple-output decision feedback at the receiving side, while downstream crosstalk is eliminated by analogous preprocessing at the transmitting side. Additionally, the issue of transmission energy allocation in frequency and among users is addressed. Assuming frequency-division duplexing, the corresponding optimization problem is formulated and solved via convex programming both for a fixed upstream–downstream band plan and for a dynamically programmable band plan. The case of power backoff as a means to reduce the impact of crosstalk on alien systems is also treated. Interestingly, the performance of the proposed methods is shown to be very close to known information theory bounds.

***Index Terms*—Broadcast channel, convex optimization, digital subscriber lines, energy allocation, interference cancellation, multiple access channel, multiuser detection, power backoff, QR decomposition, transmission optimization.**

I. Introduction

DIGITAL subscriber line (DSL) systems are rapidly gaining popularity as a broadband access technology capable of reliably delivering high data rates over telephone subscriber lines. The successful deployment of asymmetric DSL (ADSL) systems has helped reveal the potential of this technology, and current standardization efforts focus on very high-speed DSL (VDSL), which allows the use of bandwidth up to 20 MHz [1]–[5]. ADSL can reach downstream rates up to 6 Mbps, while VDSL aims to deliver asymmetric service with downstream rates up to 52 Mbps and symmetric service with rates up to 13 Mbps. Yet, several results in this paper suggest that DSL communication is still far from reaching its full potential, and that the gradual "shortening" of the loop combined with the application of advanced algorithms can realize the deployment of symmetric services with rates approaching 100 Mbps.

The current DSL system topology is shown in Fig. 1, where twisted pairs emanate from the central office (CO) and reach out to the customer premises equipment (CPE) of the DSL customers (see [6] for more details). The existing "line unbundling" regulatory framework allows for multiple service providers to share the loop plant, where each provider has physical access to the twisted pairs corresponding to their customers. However, crosstalk among the lines is a dominant impairment for DSL transmission. The current approach to control crosstalk is to restrict all DSL systems to follow certain guidelines on transmission parameters such as their power spectral density (PSD). These "spectrum management" restrictions are conservatively designed so that proper operation is guaranteed in 99% of all cases (see [7]).

Recently, major Telecom companies have embarked on a large effort to install optical network units (ONUs) at points between the CO and the CPEs. These aim to shorten the loop lengths, so that the reach and performance of DSL service are improved. The current architecture of "line unbundling" becomes impractical with the installation of ONUs, since it implies that each service provider uses an individual fiber to provide a proprietary connection to the ONU and that the ONU must be large enough to accommodate a shelf or rack for each service provider [8]. These difficulties will likely cause the evolution to "packet unbundling," where service bandwidth is leased at the *transport* layer instead of the *physical* layer (see Fig. 2). In this case, DSL transmission in the loop plant is exclusively controlled by a single entity, which allows for "coordinated" transmission/reception techniques. In the following, it is shown that such techniques eliminate the need for spectrum management rules and greatly improve the performance of VDSL.

As mentioned earlier, the dominant impairment in DSL systems is crosstalk arising from electromagnetic coupling between neighboring twisted pairs. FEXT describes the coupled signals that originate from the end opposite of the affected receiver, while near-end crosstalk (NEXT) describes the coupled signals that originate from the same end as the affected receiver. (Fig. 3 shows both NEXT and FEXT signals induced by upstream transmission of user 1.) In VDSL, the impact of NEXT from same systems is suppressed by employing frequency-division duplexing (FDD) to separate downstream and upstream transmission. Then, FEXT from VDSL systems (often called "self-FEXT") is the major performance-constraining factor, especially as the loop length becomes shorter. It should not be overlooked that non-VDSL systems induce both NEXT and

Manuscript received April 2, 2001; revised December 13, 2001. This work was supported in part by Samsung, Intel, AMD, TI, France Telecom, Telcordia, SK Telecom, and CommTech. This paper was presented in part at the 34th Asilomar Conference on Signals, Systems, and Computers, and at ICC 2001.

G. Ginis was with the Department of Electrical Engineering, Stanford University, Stanford, CA 09305 USA. He is now with the Broadband Communications Group of Texas Instruments, San Jose, CA 95124 USA (e-mail: gginis@ti.com).

J. M. Cioffi is with the Department of Electrical Engineering, Stanford University, Stanford, CA 09305 USA (e-mail: cioffi@stanford.edu).

Publisher Item Identifier S 0733-8716(02)05374-X.

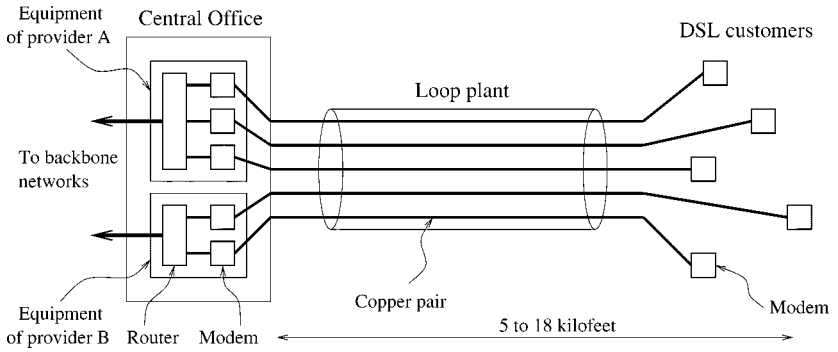

Fig. 1. Current DSL system topology.

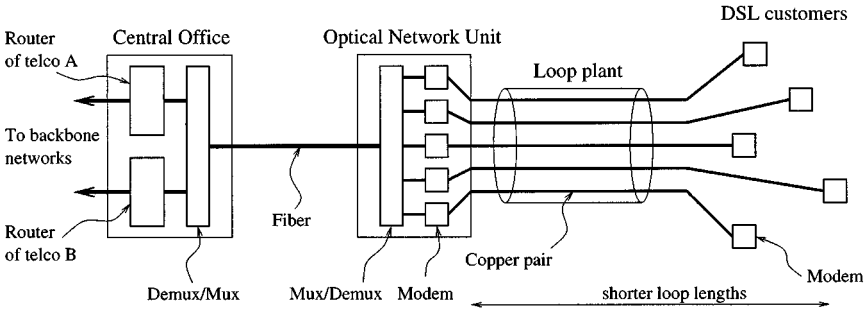

Fig. 2. Future DSL system topology.

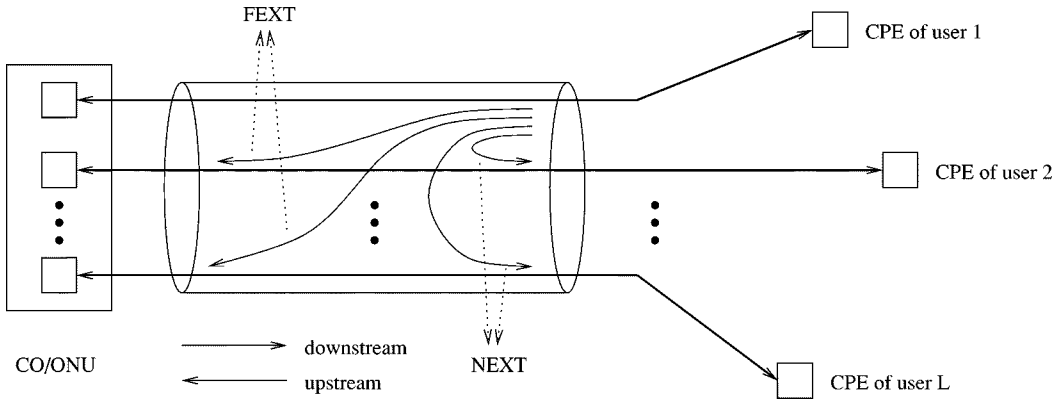

Fig. 3. DSL crosstalk environment.

FEXT, but their effect is not as severe as self-FEXT, due to the fact that they occupy a much narrower bandwidth.

The objective of *vectored transmission* (sometimes referred as "vectoring" in this paper) is to eliminate self-FEXT by treating the channel as a multiinput/multioutput (MIMO) system and employing joint signal processing of all signals at either the receiver side (for upstream transmission) or at the transmitter side (for downstream transmission). Crosstalk coupling is strongest among the twisted pairs in a binder group, therefore mitigating self-FEXT within a binder group has the biggest performance benefit. Thus, in order to obtain the maximum advantage from vectored transmission, the CO/ONU transceivers corresponding to a binder group must be colocated and controlled by a single entity. As argued earlier, this situation will become more and more common as the installation of ONUs progresses.

This paper outlines the vectored transmission technique and attempts to address several of the practical issues related to its implementation. Section II gives the channel model and defines coordinated discrete multitone (DMT) transmission, which makes it sufficient to perform crosstalk mitigation independently in each tone. Section III presents the crosstalk cancelling structures for upstream and downstream communication and discusses their relation to other known methods, while addressing some relevant practical issues. In Section IV, the issue of transmission optimization is treated, where the objective is the optimal allocation of energy across frequency and among users given a set of energy and induced crosstalk constraints. A solution to the problem of joint energy and frequency planning is also presented. Then, Section V shows corresponding simulation results. Finally, Section VI presents rate bounds obtained from information theory and compares

them against the achievable rates with vectoring. Interestingly, the proposed methods perform very close to these bounds.

The crosstalk problem has previously been addressed in [9] and [10], where MIMO minimum-mean-square-error (MMSE) linear equalizers were derived, as opposed to the decision-directed ones adopted in this paper. Reference [11] employed the singular value decomposition (similarly to [12] applied in wireless) to achieve crosstalk cancellation assuming colocation of both transmitters and receivers. Other related work includes [13] and [14], where "wider than Nyquist" transmitters were shown to provide performance advantages compared to "Nyquist-limited" ones, and [15], where crosstalk cyclostationarity (induced by transmitter synchronization) combined with oversampling were shown to result in higher signal-to-noise ratio (SNR) values.

The following notation is used throughout the paper: upper-case letters denote matrices, and bold letters denote vectors. The superscripts T and $*$ denote the transpose and conjugate transpose operations, correspondingly. The symbols $(.)_k$, and $||.||$ denote correspondingly the kth element of a vector and the square norm of a vector. The operator $\mathrm{diag}(.)$ has a different meaning depending on its argument. If the argument is a matrix, then its off-diagonal elements are zeroed. If the argument is a list of elements (or matrices), then a diagonal (or block diagonal) matrix is produced from these elements (or matrices).

II. Channel Model and DMT Transmission

The DSL channel model for the architecture of Fig. 3 is now presented. The L users are assumed to correspond to a subset of the twisted pairs of a binder group. The sampled output for a specific user for either upstream or downstream transmission depends on the present and past input symbols of both the intended user and the other crosstalking users. A block of N output samples for user i satisfies

$$\mathbf{y}_i = H^c_{i,1}\mathbf{x}^p_1 + \cdots + H^c_{i,i}\mathbf{x}^p_i + \cdots + H^c_{i,L}\mathbf{x}^p_L + \mathbf{n}_i \qquad (1)$$

where $H^c_{i,1}, \ldots, H^c_{i,L}$ are convolution matrices derived from the channel impulse response matrix, $\mathbf{y}_i$ is the vector of N output samples of receiver i, $\mathbf{x}^p_k$ is the vector of $N+\nu$ input symbols of user k, and $\mathbf{n}_i$ is the vector of N noise samples of receiver i. Evidently, ν represents the maximum memory of the transfer and crosstalk coupling functions expressed in number of samples. The noise samples represent the superposition of several noise sources such as crosstalk from neighboring DSL systems, radio frequency ingress, impulse noise, and background noise. In the following, $\mathbf{n}_i$ is considered to be white and Gaussian, and, without loss of generality, has unit variance.

Two fundamental assumptions are required in order to proceed.

- All users must employ block transmission with a CP of at least length ν (as outlined in [16]).
- Block transmission and reception at the CO/ONU must be synchronized as illustrated in the timing diagram of Fig. 4.

Given the colocation assumption, synchronized block transmission is relatively straightforward to implement, but synchronized block reception needs some more attention. The block boundaries for upstream transmission must be aligned in such a way so that the blocks of all users arrive simultaneously at the CO/ONU. This block-level synchronization must be performed during initialization, and it is analogous to the problem of synchronized uplink transmission in a wireless environment.

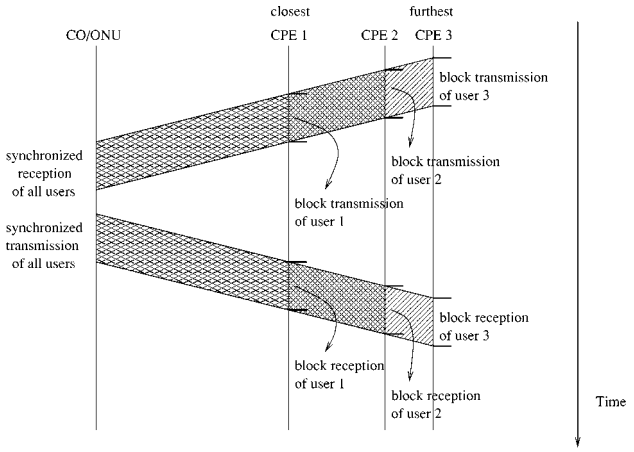

Fig. 4. Timing diagram for synchronized block transmission and reception at the CO/ONU.

Synchronization at the CO/ONU is automatically achieved when "Zipper" FDD is used (see [17]). According to this technique, a cyclic suffix (CS) is included in addition to the CP, with size larger than the channel propagation delay. "Zippering" offers the benefit of eliminating residual NEXT and near-echo resulting from "spectral leakage"at frequencies close to the upstream/downstream band edges. Nevertheless, in the remainder of this paper, the less stringent assumptions of the previous paragraph will be made, with the tacit understanding that residual NEXT and near-echo are mitigated by transmitter pulse-shaping and receiver windowing as in [18].

Taking the above into account, (1) becomes

$$\mathbf{y}_i = H_{i,1}\mathbf{x}_1 + \cdots + H_{i,i}\mathbf{x}_i + \cdots + H_{i,L}\mathbf{x}_L + \mathbf{n}_i \qquad (2)$$

where $\mathbf{x}_k$ is a vector of N input symbols of user k, and $H_{i,j}$, $i, j = 1, \ldots, L$ are circulant matrices. Combining the L users, (2) becomes

$$\mathbf{y} = H\mathbf{x} + \mathbf{n} \qquad (3)$$

where $\mathbf{y} = [\mathbf{y}_1^T\ \mathbf{y}_2^T \cdots \mathbf{y}_L^T]^T$, $\mathbf{x} = [\mathbf{x}_1^T\ \mathbf{x}_2^T \cdots \mathbf{x}_L^T]^T$, $\mathbf{n} = [\mathbf{n}_1^T\ \mathbf{n}_2^T \cdots \mathbf{n}_L^T]^T$, and H is a matrix whose (i, j) block is $H_{i,j}$. The noise covariance matrix is assumed to be $R_{\mathbf{nn}} = I$.

Applying the discrete Fourier transform (DFT) modulation principle of [19] and [16], an inverse discrete Fourier transform (IDFT) operation is performed on each transmitted data block (prior to appending the CP), and a DFT operation is performed on each received data block (after discarding the CP)

$$\begin{aligned}\mathbf{Y} &= Q_{m\mathrm{DFT}} H Q_{m\mathrm{IDFT}}\mathbf{X} + Q_{m\mathrm{DFT}}\mathbf{n} \\ &= \Lambda\mathbf{X} + \mathbf{N}'\end{aligned} \qquad (4)$$

where

$$\mathbf{Y} = \left[\mathbf{Y}_1^T\mathbf{Y}_2^T \cdots \mathbf{Y}_L^T\right]^T = Q_{m\mathrm{DFT}}\mathbf{y} \qquad (5)$$

$$\mathbf{x} = Q_{m\mathrm{IDFT}}\left[\mathbf{X}_1^T\mathbf{X}_2^T \cdots \mathbf{X}_L^T\right]^T = Q_{m\mathrm{IDFT}}\mathbf{X} \qquad (6)$$

$$\mathbf{N}' = \left[\mathbf{N}_1'^T\mathbf{N}_2'^T \cdots \mathbf{N}_L'^T\right]^T = Q_{m\mathrm{DFT}}\mathbf{n} \qquad (7)$$

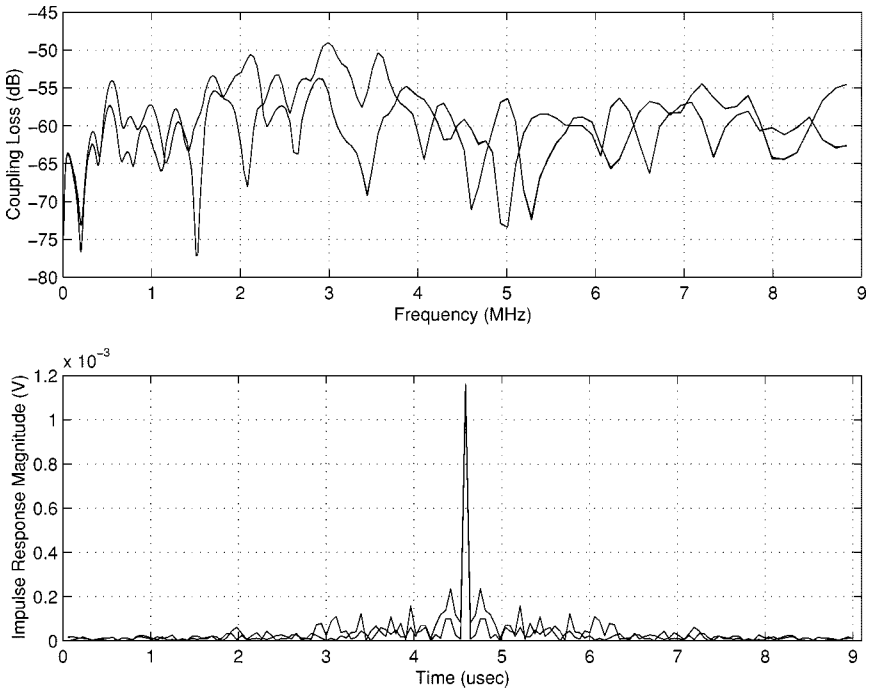

Fig. 5. FEXT frequency response measurements and corresponding impulse responses.

$$Q_{m\mathrm{IDFT}} = \mathrm{diag}\left(\overbrace{Q_{\mathrm{IDFT}}, Q_{\mathrm{IDFT}}, \ldots, Q_{\mathrm{IDFT}}}^{L}\right) \tag{8}$$

with Q_{IDFT} the $N \times N$ IDFT matrix, $Q_{\mathrm{DFT}} = Q^*_{\mathrm{IDFT}}$ the corresponding DFT matrix, and $Q_{m\mathrm{DFT}} = Q^*_{m\mathrm{IDFT}}$. Also, $\mathbf{Y}_k$, $\mathbf{X}_k$, $\mathbf{N}'_k$ each contain N samples corresponding to user k, $R_{\mathbf{N}'\mathbf{N}'} = I$, and Λ is a matrix whose (i, j) block is the diagonal matrix $\Lambda_{i,j} = Q_{\mathrm{DFT}} H_{i,j} Q_{\mathrm{IDFT}}$.

Therefore, (4) gives a channel description, where the samples are stacked in groups corresponding to users, and each of the groups contains samples corresponding to tones. It is desirable to reorganize these samples, so that they are stacked in groups corresponding to tones, and each of these groups contains samples corresponding to different users. To this end, a permutation matrix P having NL rows and NL columns is defined, which is composed of the $N \times N$ blocks $P_{i,j}$ where $i, j = 1, \ldots, L$. The block $P_{i,j}$ contains all zeros, except for a one at position (j, i). Some inspection reveals that, when matrix P is right-multiplied with a vector of size NL, it essentially reorders its elements from L groups of N components into N groups of L components. Also, note that $P^{-1} = P^* = P$. Applying this reordering operation to both the transmitter and the receiver samples yields

$$\begin{aligned}\mathbf{Z} &= P\Lambda P P\mathbf{X} + P\mathbf{N}' \\ &= P\Lambda P\mathbf{U} + \mathbf{N} \\ &= T\mathbf{U} + \mathbf{N}\end{aligned} \tag{9}$$

where

$$\mathbf{Z} = \left[\mathbf{Z}_1^T \mathbf{Z}_2^T \cdots \mathbf{Z}_N^T\right]^T = P\mathbf{Y} \tag{10}$$

$$\mathbf{U} = \left[\mathbf{U}_1^T \mathbf{U}_2^T \cdots \mathbf{U}_N^T\right]^T = P\mathbf{X} \tag{11}$$

$$\mathbf{N} = \left[\mathbf{N}_1^T \mathbf{N}_2^T \cdots \mathbf{N}_N^T\right]^T = P\mathbf{N}' \tag{12}$$

$$T = P\Lambda P = \mathrm{diag}\left(\overbrace{T_1, T_2, \ldots, T_N}^{N}\right) \tag{13}$$

with $R_{\mathbf{N}\mathbf{N}} = I$. Finally, (9) becomes

$$\mathbf{Z}_i = T_i \mathbf{U}_i + \mathbf{N}_i, \qquad i = 1, \ldots, N. \tag{14}$$

Therefore, $\mathbf{Z}_i$, $\mathbf{U}_i$, and $\mathbf{N}_i$ contain the received samples, transmitted symbols, and noise samples of all users corresponding to tone i, and T_i fully characterizes MIMO transmission within tone i. In the following, a distinction between upstream and downstream will be made by adopting the notation $T_{i,\mathrm{up}}$ and $T_{i,\mathrm{down}}$.

Equation (14) indicates that crosstalk cancellation can be performed independently in each tone. Therefore, as shown in the next section, an array of canceller blocks can be employed at the CO/ONU to remove crosstalk within each tone for upstream communication. Similarly, precoder blocks can be used at the CO/ONU to predistort the transmitted signals within each tone, so that the received signals are crosstalk-free. However, determining the parameters of the canceller/precoder blocks relies on perfect channel matrix and noise covariance matrix knowledge at the CO/ONU. This is fairly reasonable for DSL, since the twisted pair channels are stationary and systems can afford the luxury of training-based channel identification during initialization.

A. Practical Issues for the VDSL Environment

A few comments are now made about the CP and synchronization assumptions with regard to the VDSL environment. The additional requirement of having a CP longer than the memory of both the transfer and the crosstalk coupling functions can be satisfied without suffering an excessive loss. Fig. 5 shows FEXT coupling measurements for loops with length of

1640 ft. Since only magnitude data is provided, linear phase is assumed in order to derive the impulse responses, and it is found that 99.9% of the signal energy is contained within 9 μs. With a DMT block size of 4096 samples and sampling rate of 17.664 MHz, this corresponds to 159 samples. Therefore, the currently proposed CP length of 320 samples (corresponding to a 7.8% loss) is more than adequate, and it is expected that this will remain true with any typical FEXT coupling function.

The average delay of a typical twisted pair is approximately 1.5 μs/kft (see [20]). Given that VDSL loops usually have lengths shorter than 6000 ft, and with the previous DMT assumptions, the propagation delay corresponds to fewer than 160 samples. Therefore, even if "Zippering" is used, the length of the CP plus the CS does not exceed the proposed 320 samples. In cases where the channel has unusually long memory, a MIMO time-domain-equalizer may be used at the CO/ONU as described in [21]. Although this technique applies to upstream communication only, a MIMO extension of the precoder proposed in [22] may be utilized for downstream communication.

III. Crosstalk Cancellation via QR Decomposition

Starting from (14), the methods to remove the crosstalk within each tone are now described first for upstream and then for downstream communication. In the following, the matrices $T_{i,\,\mathrm{up}}$, $T_{i,\,\mathrm{down}}$ are assumed to be nonsingular (the validity of this claim and the consequences of ill conditioning will be examined later).

A. Upstream

For upstream transmission, the colocation of the CO/ONU transceiver equipment gives the opportunity to perform joint signal processing of the received samples. The computation of the QR decomposition of matrix $T_{i,\,\mathrm{up}}$ yields

$$T_{i,\,\mathrm{up}} = Q_i R_i \tag{15}$$

where Q_i is a unitary matrix and R_i is an upper triangular matrix. If the received samples are "rotated/reflected" by Q_i^*, then (14) becomes

$$\tilde{\mathbf{Z}}_i = Q_i^* \mathbf{Z}_i \tag{16}$$

$$= R_i \mathbf{U}_i + \tilde{\mathbf{N}}_i \tag{17}$$

where $\tilde{\mathbf{N}}_i = Q_i^* \mathbf{N}_i$ has an identity covariance matrix. Since R_i is upper triangular and $\tilde{\mathbf{N}}_i$ has uncorrelated components, the input $\mathbf{U}_i$ can be recovered by back-substitution combined with symbol-by-symbol detection. Thus, a decision feedback structure is derived with the feedforward matrix being Q_i^* and the feedback matrix being $I - R_i$. The detection of the kth element of $\mathbf{U}_i$ is expressed as

$$\left(\hat{\mathbf{U}}_i\right)_k = \text{decode}\left[\frac{1}{r_{k,k}^i}\left(\tilde{\mathbf{Z}}_i\right)_k - \sum_{j=k+1}^{L} \frac{r_{k,j}^i}{r_{k,k}^i}\left(\hat{\mathbf{U}}_i\right)_j\right], \quad k = L, L-1, \ldots, 1 \tag{18}$$

where $r_{k,\,j}^i$ is the $(k,\,j)$ element of R_i. Assuming that the previous decisions are correct, crosstalk is completely cancelled,

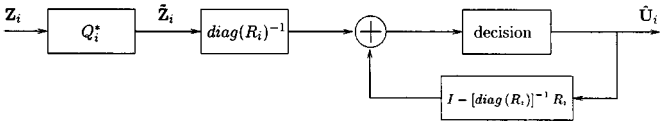

Fig. 6. Canceller block.

and L "parallel" channels are created within each tone. The detection SNR of user k on tone i then equals

$$\mathrm{SNR}_k^i = |r_{k,k}^i|^2 \mathcal{E}_{k,\,\mathrm{up}}^i \tag{19}$$

where $\mathcal{E}_{k,\,\mathrm{up}}^i$ is the energy of $(\mathbf{U}_i)_k$.

The operations described above define the canceller block corresponding to a single tone, which is shown in Fig. 6. Combining the canceller blocks of all tones, and taking into account DMT transmission, the system for upstream vectored-DMT transmission is obtained as in Fig. 7.

Note that the above technique can be combined with coding, where each user employs its own code. In that case, (18) indicates that decoding the kth user requires that users $k+1$ through L have already been decoded. Since decoding typically involves a delay, it is seen that the symbols of the kth user must be buffered, until users $k+1$ through L have been decoded. Evidently, users with smaller indices are characterized by higher latency.

B. Downstream

For downstream transmission, joint signal processing of the transmitted symbols is allowed. The QR decomposition of $T_{i,\,\mathrm{down}}^T$ results in

$$T_{i,\,\mathrm{down}}^T = Q_i R_i \tag{20}$$

where again Q_i is a unitary matrix and R_i is an upper triangular matrix. Assuming that the symbols are "rotated/reflected" by Q_i^{T*} prior to being transmitted

$$\mathbf{U}_i = Q_i^{T*} \mathbf{U}_i'. \tag{21}$$

So, with the choice of

$$\mathbf{U}_i' = R_i^{-T} \mathrm{diag}(R_i^T) \tilde{\mathbf{U}}_i \tag{22}$$

crosstalk-free reception is achieved, where the transmitted symbols in tone i are the elements of $\tilde{\mathbf{U}}_i$. However, this operation may cause undesired energy increase, so, utilizing the concept of Tomlinson–Harashima precoding (see [24] and [25]), it is replaced by

$$(\mathbf{U}_i')_k = \Gamma_{M_{i,\,k}}\left[\left(\tilde{\mathbf{U}}_i\right)_k - \sum_{j=1}^{k-1} \frac{r_{j,k}^i}{r_{k,k}^i}(\mathbf{U}_i')_j\right], \quad k = 1, 2, \ldots, L. \tag{23}$$

The following operation is performed at the receiver

$$\left(\hat{\mathbf{Z}}_i\right)_k = \Gamma_{M_{i,\,k}}\left[\frac{(\mathbf{Z}_i)_k}{r_{k,k}^i}\right], \qquad k = 1, 2, \ldots, L \tag{24}$$

where $\Gamma_{M_{i,\,k}}$ is defined as

$$\Gamma_{M_{i,\,k}}[x] = x - M_{i,\,k} d \left\lfloor \frac{x + \frac{M_{i,\,k} d}{2}}{M_{i,\,k} d} \right\rfloor \tag{25}$$

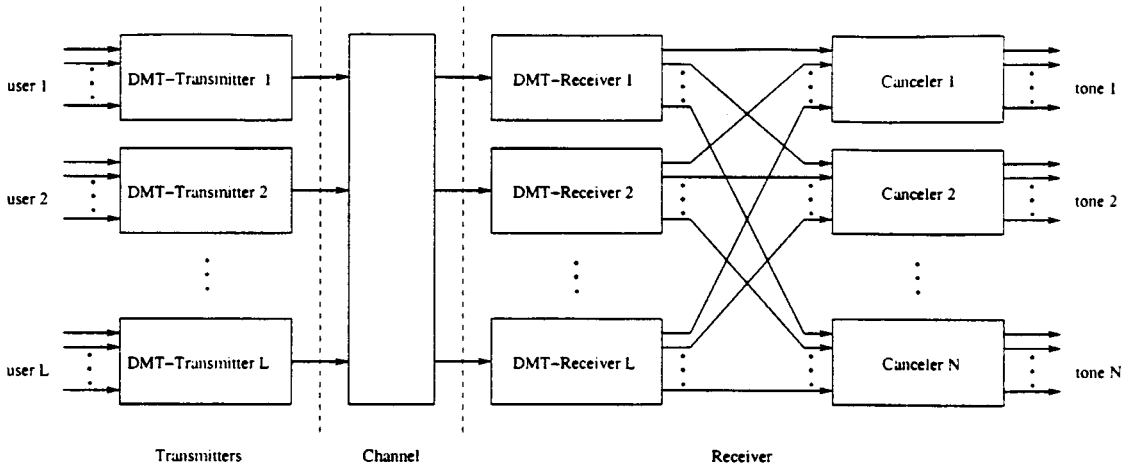

Fig. 7. Vectored-DMT for upstream communication.

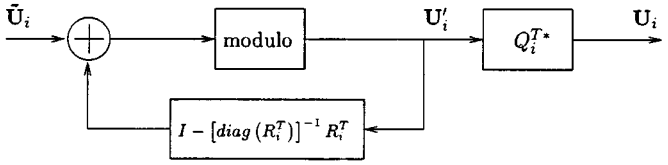

Fig. 8. Precoder block.

and $M_{i,k}$ is the constellation size of user k on tone i, while d is the constellation point spacing. (If x is complex, then $\Gamma_{M_{i,k}}[x] = \Gamma_{\sqrt{M_{i,k}}}[\Re(x)] + j\Gamma_{\sqrt{M_{i,k}}}[\Im(x)]$.) It is shown in [23] that these operations result in

$$\hat{\mathbf{Z}}_i = \tilde{\mathbf{U}}_i + \left[\mathrm{diag}(R_i^T)\right]^{-1} \mathbf{N}_i \tag{26}$$

which implies crosstalk-free reception. The detection SNR of user k on tone i equals

$$\mathrm{SNR}_k^i = |r_{k,k}^i|^2 \mathcal{E}_{k,\,\mathrm{down}}^i \tag{27}$$

where $\mathcal{E}_{k,\,\mathrm{down}}^i = \tilde{\mathcal{E}}_k^i$ is the energy of $(\tilde{\mathbf{U}}_i)_k$.

The MIMO precoder described above corresponds to a single tone and is shown in Fig. 8. Combining the precoders of all tones and including the DMT transmitters and receivers, the vectored-DMT system for downstream transmission is obtained as in Fig. 9.

This technique can easily be combined with coding, where each user employs its own code. Coding only needs to be applied independently on the symbols of each user prior to the precoding operations.

C. Some Comments About Cancellation via QR

An alternative derivation of the crosstalk cancellation structures described above is given in [26], where it is proved that these are special cases of the zero-forcing (ZF) version of the generalized decision-feedback-equalizer (GDFE) (see [27]). The GDFE is a MIMO extension of the well-known DFE employed for intersymbol-interference (ISI) equalization.

It can be observed that the upstream crosstalk cancellation scheme is similar to the V-BLAST architecture proposed for wireless communication with multiple antennas (see [28] and [29]). Actually, based on the equivalency between V-BLAST and GDFE (shown in [30]), it is deduced that the upstream QR cancellation method is identical to the processing steps of BLAST. The main difference lies in the fact that, instead of twisted pairs suffering from crosstalk, there are multiple antennas receiving the signals of multiple transmitting antennas. Also, it is worth noting that the decision-feedback multiuser detectors described in [31] share several similarities with the QR cancellation scheme.

Under the assumption that transmit and receive filtering at the CO/ONU and at the CPEs is identical, and noise within a tone has the same statistics for all users, the reciprocity property for twisted pair transmission implies that $T_{i,\,\mathrm{up}} = T_{i,\,\mathrm{down}}^T$. In that case, (15) and (20) give the QR decomposition of the same matrix.

For the upstream channel, it is *always* true, regardless of the loop topology, that the diagonal element of a column of T_i is larger in magnitude than the off-diagonal elements of the same column. In other words, the diagonal elements of T_i dominate "column-wise." This occurs because in upstream transmission the crosstalk coupled signal originating from a specific transmitter can never exceed the "directly" received signal of the same transmitter, and typically the magnitude difference is more than 20 dB. This can be verified in Fig. 10, which refers to a pessimistic case, where a 500-ft pair neighbors a 6000-ft pair (and both consist of AWG-26 copper wire). The insertion losses are shown together with the FEXT coupling losses, assuming upstream transmission and colocation at the CO/ONU. The data were obtained using the standard models adopted by the T1E1.4 committee [1]. Clearly, the insertion loss of a signal is always smaller than the coupling loss that it experiences when it propagates into a neighboring pair. It is worth stressing that this condition is not equivalent to saying that the crosstalk signals are weak. Notice that, for the example of Fig. 10, the crosstalk coupling into loop 2 is much stronger than the transfer function of loop 2 at all frequencies above 1.7 MHz.

Visualizing the columns of T_i in vector space, it is seen that the columns are almost orthogonal to each other, which implies that Q_i is close to being an identity matrix. Thus, the magnitudes of the diagonal elements of R_i do not differ significantly

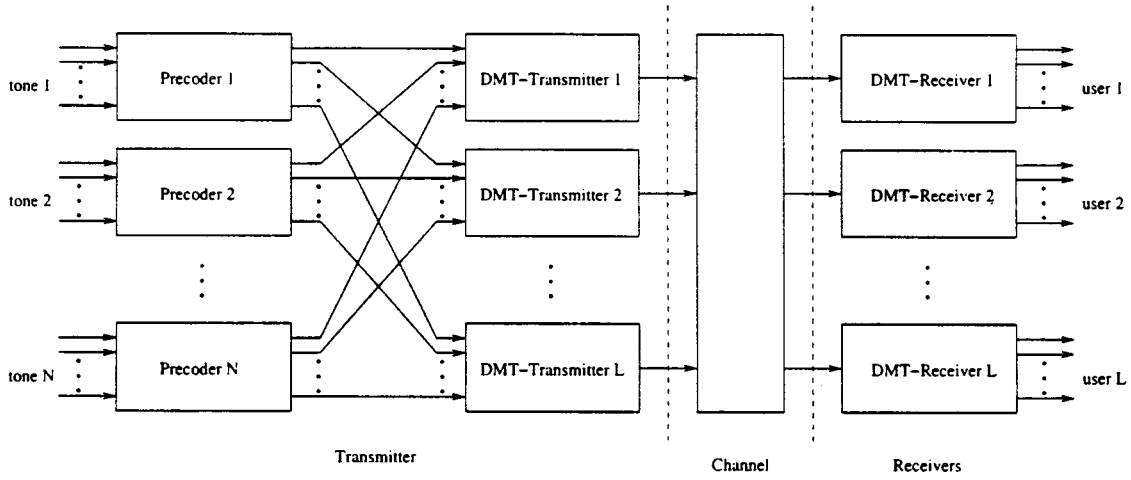

Fig. 9. Vectored-DMT system for downstream communication.

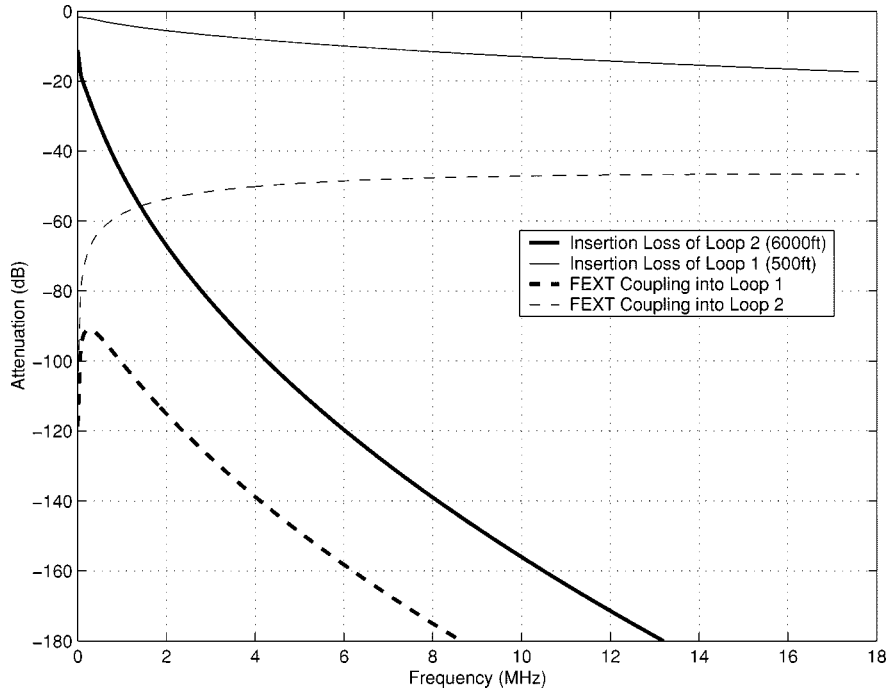

Fig. 10. Insertion loss and FEXT coupling loss for an extreme loop topology.

from those of the diagonal elements of T_i, which indicates that QR cancellation performs almost as well as perfect crosstalk removal. This is illustrated in Fig. 11 for a two user case, where $\mathbf{t}_1, \mathbf{t}_2$ are the columns of T_i, $\mathbf{q}_1, \mathbf{q}_2$ are the columns of Q_i, r_{mn} is the (m, n) element of R, and $|r_{11}| = ||\mathbf{t}_1||$. The fact that $\mathbf{t}_1$, $\mathbf{t}_2$ are close to orthogonal to the axes implies that $|r_{22}| \approx ||\mathbf{t}_2||$. As shown in the figure, this holds for both possible detection orderings. Appendix I generalizes this observation for multiple users and derives appropriate bounds for $|r_{kk}|$.

Fig. 12 shows the upstream *channel* SNRs for the same loop topology as in Fig. 10, either assuming that no crosstalk exists, or that crosstalk is cancelled by vectored transmission. (Channel SNR is defined as equal to the SNR with unit transmission energy.) The background noise is white with PSD equal to -140 dBm/Hz. Since the QR decompositions differ when the columns of T_i are swapped, the two possible orderings are displayed. Clearly, the plots corresponding to the same loop overlap almost perfectly, which means that QR cancellation is as good as having no crosstalk, and that the impact of ordering can be ignored. Also, this serves as evidence that the crosstalk ZF criterion is fairly adequate, and employing an MMSE criterion will not yield noticeable improvement.

All the previous arguments were made for upstream transmission, but they can easily be extended to downstream transmission by starting with the observation that the crosstalk signals at a specific receiver can never exceed in magnitude the "directly" received signal. (Alternatively, the same conclusions can be reached by using the transpose relationship between the upstream and downstream channel matrices, which in most practical situations is approximately true.) In this case, the diagonal element of a row of T_i is *always* larger in magnitude than the off-diagonal elements of the same row. Again, it should be

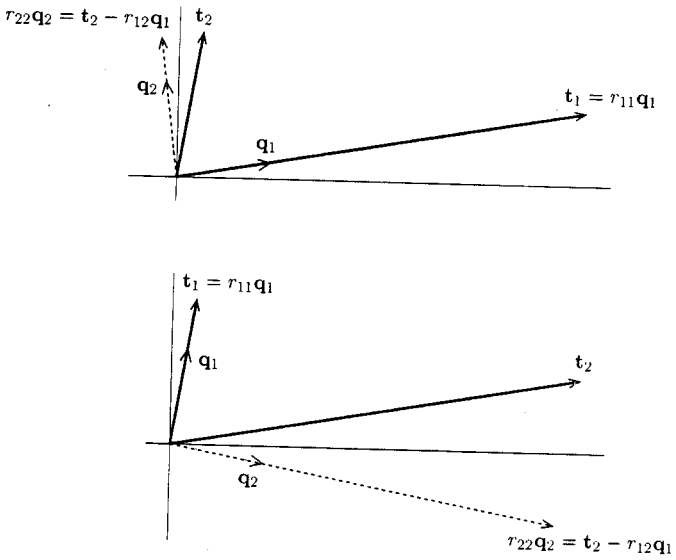

Fig. 11. Illustration of QR decomposition for the two possible orderings.

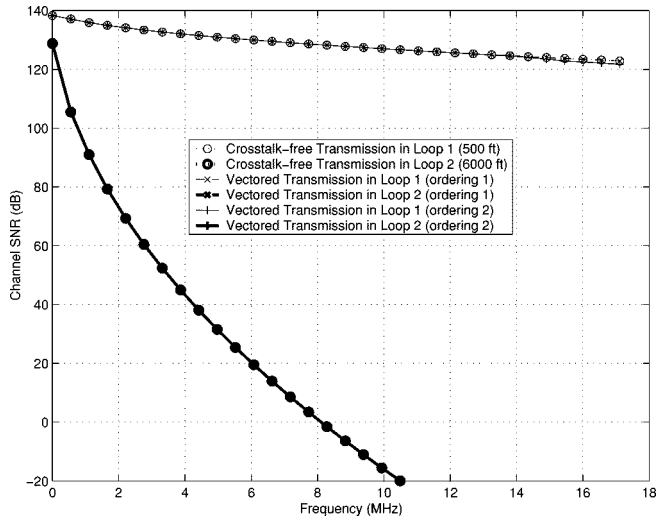

Fig. 12. Channel SNRs in crosstalk-free environment and in crosstalk environment with vectoring (shown for the two possible orderings).

stressed that this condition is not equivalent to saying that the crosstalk signals are weak, and therefore the modulo operation is absolutely necessary during precoding, in order to prevent energy increase.

D. Practical Considerations

The computational cost incurred by the QR cancellation is decomposed into the cost of the QR decompositions and the cost associated with signal processing. DSL channels are stationary, so the QR decompositions need to be computed infrequently (during initialization). Generally, this requires $\mathcal{O}(L^3)$ flops per tone (e.g., using the Householder transform as in [32]), but it can be greatly reduced by taking advantage of the crosstalk environment characteristics. It is known that the crosstalk noise in a pair originates mostly from just three or four neighboring pairs, which implies that a typical T_i matrix is practically sparse with only three or four relatively large off-diagonal elements per row. Therefore, approximating T_i as a sparse matrix, Givens rotations can be employed to triangularize T_i with a reduced cost of $\mathcal{O}(L^2)$ flops. The real-time computational burden due to the canceller and precoder blocks can also be reduced by employing Givens rotations. It is not hard to show that the operations of (16) and (21) require only $\mathcal{O}(L)$ flops per tone.

Although the assumption of perfect channel matrix knowledge is fairly reasonable in the given environment, it is still worth examining the effects of channel estimation errors. Let the estimated upstream channel matrix for tone i be

$$\hat{T}_{i,\,\mathrm{up}} = T_{i,\,\mathrm{up}} + E_i \tag{28}$$

where E_i is the channel estimation error. Then, performing the QR decomposition with the reciprocity assumption gives

$$\hat{T}_{i,\,\mathrm{up}} = \hat{Q}_i \hat{R}_i - E_i \tag{29}$$

$$\hat{T}_{i,\,\mathrm{down}} = \hat{R}_i^T \hat{Q}_i^T - E_i^T \tag{30}$$

where $\hat{Q}_i$, $\hat{R}_i$ are the QR factor estimates. Starting from (16), the effect on upstream communication can be computed

$$\begin{aligned}
\tilde{\mathbf{Z}}_i &= \left(\hat{R}_i - \hat{Q}_i^* E_i\right)\mathbf{U}_i + \hat{Q}_i^* \mathbf{N}_i \Rightarrow \\
\hat{\mathbf{U}}_i &= dec\left[\mathbf{U}_i - \left[\mathrm{diag}\left(\hat{R}_i\right)\right]^{-1} \hat{Q}_i^* E_i \mathbf{U}_i \right. \\
&\qquad \left. + \left[\mathrm{diag}\left(\hat{R}_i\right)\right]^{-1} \hat{Q}_i^* \mathbf{N}_i\right] \\
&= dec\left[\left\{1 - \left[\mathrm{diag}\left(\hat{R}_i\right)\right]^{-1} \mathrm{diag}\left(\hat{Q}_i^* E_i\right)\right\}\mathbf{U}_i \right. \\
&\qquad - \left[\mathrm{diag}\left(\hat{R}_i\right)\right]^{-1}\left[\hat{Q}_i^* E_i - \mathrm{diag}\left(\hat{Q}_i^* E_i\right)\right]\mathbf{U}_i \\
&\qquad \left. + \left[\mathrm{diag}\left(\hat{R}_i\right)\right]^{-1} \hat{Q}_i^* \mathbf{N}_i\right]
\end{aligned} \tag{31}$$

where $dec[.]$ acts on the elements of a vector. So, the estimation errors impact transmission by introducing a "bias" in the detection [first term in (31)] and also by resulting in some residual crosstalk [second term in (31)]. A similar analysis can be applied for downstream communication, but modulo arithmetic complicates the expressions. Ignoring the modulo operations and employing (21), (22) gives

$$\begin{aligned}
\mathbf{Z}_i &= \left(\hat{R}_i^T \hat{Q}_i^T - E_i^T\right)\mathbf{U}_i + \mathbf{N}_i \\
&= \mathrm{diag}\left(\hat{R}_i^T\right)\tilde{\mathbf{U}}_i - E_i^T \hat{Q}_i^{T*} \mathbf{U}_i' + \mathbf{N}_i \Rightarrow \\
\hat{\mathbf{Z}}_i &= \tilde{\mathbf{U}}_i - \left[\mathrm{diag}\left(\hat{R}_i^T\right)\right]^{-1} E_i^T \hat{Q}_i^{T*} \hat{R}_i^{-T} \mathrm{diag}\left(\hat{R}_i^T\right)\tilde{\mathbf{U}}_i \\
&\qquad + \left[\mathrm{diag}\left(\hat{R}_i^T\right)\right]^{-1} \mathbf{N}_i.
\end{aligned} \tag{32}$$

Just as before, the effects of the estimation errors can be separated into a detection bias term and a residual crosstalk term.

Equations (31) and (32) reveal that the impact of channel estimation errors is aggravated, when any of the diagonal elements of $\hat{R}_i$ is small. Although channel matrix singularity is almost impossible in the DSL environment, an ill-conditioned channel (implying small diagonal elements) cannot be ruled out, thus increasing the impact of channel estimation errors and posing several computational problems. Such cases arise in high

frequencies (e.g., in loop topologies similar to that of Fig. 10) or in the presence of bridged taps. Nevertheless, the energy allocation algorithms proposed in Section IV prevent the occurrence of such phenomena by not allowing transmission in frequencies where the diagonal elements of R_i are small.

Evidently, vectored-DMT is successful in cancelling self-FEXT. One could argue that self-NEXT at the CO/ONU side can also be cancelled through the use of "NEXT-cancellers" operating similarly to echo-cancellers. In that case, upstream transmission is essentially crosstalk-free, which hints that downstream transmission may occupy the whole band without any impact on upstream. However, downstream transmission in the bands employed for upstream still suffers from self-NEXT. It has been observed through simulations that (unless the self-NEXT coupling is very weak) the performance benefits of allowing downstream transmission in the whole band are minuscule. In the following, the use of FDD is assumed for the separation of downstream and upstream transmission, thus, no NEXT-cancellers are needed.

IV. Transmission Optimization

Methods to optimize transmission are now presented, where the objective is the maximization of a weighted data rate sum. These methods refer to the problems of energy allocation in frequency, energy allocation in frequency while observing constraints on induced crosstalk, and energy allocation combined with upstream/downstream frequency selection.

A. Energy Allocation

The optimization objective is the maximization of the weighted sum of the data rates of all users

$$\max \sum_{k=1}^{L} a_k R_k \tag{33}$$

where $a_k \geq 0$ is the weight assigned to the kth user and R_k is the achievable data rate of the kth user, which may refer to either the upstream or the downstream direction. In order to compute the data rate, the gap approximation is employed (see [33]). Taking into account the fact that vectoring essentially "diagonalizes" the channel (and assuming no error propagation in upstream), the upstream and downstream achievable rates are obtained

$$R_{k,\,\mathrm{up}} = \sum_{i \in \mathcal{N}_{\mathrm{up}}} \frac{1}{2} \log_2 \left(1 + \frac{|r^i_{k,k}|^2 \mathcal{E}^i_{k,\,\mathrm{up}}}{\Gamma} \right) \tag{34}$$

$$R_{k,\,\mathrm{down}} = \sum_{i \in \mathcal{N}_{\mathrm{down}}} \frac{1}{2} \log_2 \left(1 + \frac{|r^i_{k,k}|^2 \mathcal{E}^i_{k,\,\mathrm{down}}}{\Gamma} \right) \tag{35}$$

where Γ is defined as the transmission gap and depends on the probability of error requirement, the coding gain, and the required margin. Also, $\mathcal{N}_{\mathrm{up}}$ and $\mathcal{N}_{\mathrm{down}}$ are the sets of upstream and downstream tone indices correspondingly, which depend on the FDD plan. The assumption of no error propagation is justified given that errors in DSL are rather infrequent. Also, it should be noted that error propagation is not a "catastrophic" event (as in DFEs for ISI mitigation), since it always terminates when all users in (18) have been decoded.

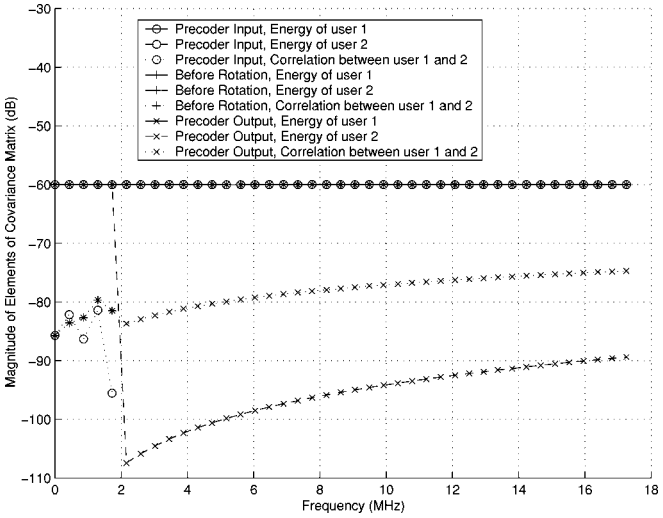

Fig. 13. Magnitude of elements of covariance matrices of precoder samples.

The parameters with respect to which optimization takes place are $\mathcal{E}^i_{k,\,\mathrm{up}}$ for upstream, and $\mathcal{E}^i_{k,\,\mathrm{down}}$ for downstream transmission, and these are constrained by limits on the transmitted energy. In upstream transmission, the total transmit energy is constrained by

$$\sum_{i \in \mathcal{N}_{\mathrm{up}}} \mathcal{E}^i_k \leq \mathcal{E}_{k,\,\mathrm{up}} \tag{36}$$

where $\mathcal{E}^i_k$ is the energy of $(\mathbf{U}_i)_k$ in (17), and $\mathcal{E}_{k,\,\mathrm{up}}$ is the maximum allowed upstream transmitted energy of user k. Since $\mathcal{E}^i_{k,\,\mathrm{up}} = \mathcal{E}^i_k$ [see (19)], it is deduced that

$$\sum_{i \in \mathcal{N}_{\mathrm{up}}} \mathcal{E}^i_{k,\,\mathrm{up}} \leq \mathcal{E}_{k,\,\mathrm{up}}. \tag{37}$$

In downstream transmission, the total transmit energy constraint is expressed as

$$\sum_{i \in \mathcal{N}_{\mathrm{down}}} \mathcal{E}^i_k \leq \mathcal{E}_{k,\,\mathrm{down}} \tag{38}$$

where $\mathcal{E}^i_k$ is the energy of $(\mathbf{U}_i)_k$ in (21), and $\mathcal{E}_{k,\,\mathrm{down}}$ is the maximum allowed downstream transmitted energy of user k. Unfortunately, this constraint does not translate directly to a constraint for $\tilde{\mathcal{E}}^i_k = \mathcal{E}^i_{k,\,\mathrm{down}}$ [see (27)], due to the nonlinear precoding operation of (23).

However, simulation results for the previously defined extreme loop topology indicate that the covariance matrix of $\mathbf{U}_i$ can be approximated fairly accurately by the covariance matrix of $\tilde{\mathbf{U}}_i$ at all tones. For simulation purposes it was assumed that the transmission PSD is flat at -60 dBm/Hz, the noise PSD is flat at -140 dBm/Hz, and the transmission gap is 12 dB. Thus, an integer bit distribution was derived, where the maximum number of bits per tone was 12. The precoder was simulated in the time domain, and the sample covariance matrices of $\tilde{\mathbf{U}}_i$, $\mathbf{U}'_i$, and $\mathbf{U}_i$ were computed with 10 000 iterations for a number of tones. Fig. 13 shows the elements (1, 1), (2, 2), and (1, 2) of these covariance matrices. It is seen that user 1 transmits data on all frequencies, while user 2 does not actually transmit any data at frequencies above 2 MHz. At frequencies below 2 MHz, the correlation between the users is very small.

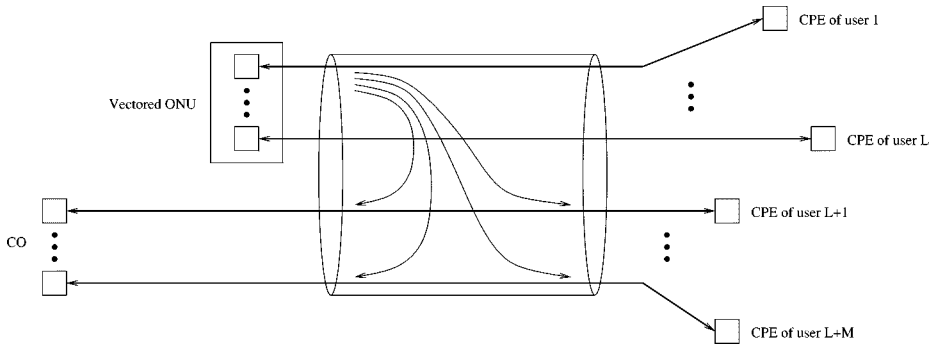

Fig. 14. DSL system topology with co-existence of CO and ONU.

At frequencies higher than 2 MHz, the rotation/reflection operation means that the precoder output of user 2 has some energy; however, the correlation still remains small. At all frequencies, the energy increase due to precoding is indiscernible.

Therefore, it is seen that the precoder does not result in considerable correlation between the transmitted signals of different users. It is reasonable to assume that this result holds generally, since the simulated loops correspond to a worst case situation with regard to the crosstalk coupling.

Therefore, the approximation $\mathcal{E}_k^i \approx \tilde{\mathcal{E}}_k^i = \mathcal{E}_{k,\,\mathrm{down}}^i$ is made, and (38) for downstream becomes

$$\sum_{i\in\mathcal{N}_{\mathrm{down}}} \mathcal{E}_{k,\,\mathrm{down}}^i \le \mathcal{E}_{k,\,\mathrm{down}}. \tag{39}$$

With this in mind, it is seen that the energy allocation problem of (33) becomes independent for each user, and thus the a_k weights are irrelevant in this scenario. The optimization problem for each transmission direction is broken into k waterfilling problems expressed by

$$\max \quad \sum_{i\in\mathcal{N}_{\mathrm{up}}} \frac{1}{2}\log_2\left(1+\frac{|r_{k,\,k}^i|^2\mathcal{E}_{k,\,\mathrm{up}}^i}{\Gamma}\right) \tag{40}$$

$$\text{subject to} \quad \sum_{i\in\mathcal{N}_{\mathrm{up}}} \mathcal{E}_{k,\,\mathrm{up}}^i \le \mathcal{E}_{k,\,\mathrm{up}} \tag{41}$$

and by

$$\max \quad \sum_{i\in\mathcal{N}_{\mathrm{down}}} \frac{1}{2}\log_2\left(1+\frac{|r_{k,\,k}^i|^2\mathcal{E}_{k,\,\mathrm{down}}^i}{\Gamma}\right) \tag{42}$$

$$\text{subject to} \quad \sum_{i\in\mathcal{N}_{\mathrm{down}}} \mathcal{E}_{k,\,\mathrm{down}}^i \le \mathcal{E}_{k,\,\mathrm{down}}. \tag{43}$$

Solutions to these problems are easy to derive and simulation results are shown in Section V-A.

Specifically for downstream transmission, a constraint on the total transmitted energy of all users could also be relevant

$$\sum_{k=1}^{L}\sum_{i\in\mathcal{N}_{\mathrm{down}}} \mathcal{E}_{k,\,\mathrm{down}}^i \le \mathcal{E}. \tag{44}$$

Nevertheless, individual energy constraints are more realistic in DSL, since they correspond to power limitations of the analog front ends of the modems. Therefore, a total energy constraint is not pursued any further.

B. Energy Allocation With Power Backoff

As explained previously, all users in vectored transmission correspond to a group of neighboring twisted pairs. This does not preclude the operation of other "alien" DSL systems in neighboring twisted pairs, which on one hand cause crosstalk into the vectored systems and on the other hand suffer from crosstalk originating from the vectored systems. The current approach in dealing with this problem is to impose limits on the transmitted PSDs, so that the performance of systems is not excessively affected by crosstalk.

Additionally, VDSL systems suffer from the fact that upstream signals on short lines detrimentally affect upstream performance on long lines (similarly to the near–far situation in wireless communications). In order to avoid imposing an overly restrictive universal PSD mask, power backoff methods have been proposed (see [34]), which effectively make the PSD mask dependent on the loop length of the specific user. An alternative approach to control this effect is the concept of iterative waterfilling [35].

A similar scenario, where the downstream communication of neighboring DSL systems may suffer considerably is shown in Fig. 14. Note that this situation will occur increasingly often as the installation of ONUs progresses, while twisted pair connections to the COs remain.

Vectoring combined with full channel matrix knowledge can prove effective in limiting the crosstalk induced by vectored systems, without resorting to the introduction of a universal PSD mask or the use of power backoff methods (which do not take into account knowledge about crosstalk coupling resulting from matrix channel identification).

Equation (9) can be augmented to include the received samples of alien systems

$$\begin{bmatrix}\mathbf{Z}\\ \mathbf{Z}_n\end{bmatrix} = \begin{bmatrix}T & C_n\\ C & T_n\end{bmatrix}\begin{bmatrix}\mathbf{U}\\ \mathbf{U}_n\end{bmatrix} + \begin{bmatrix}\mathbf{N}\\ \mathbf{N}_n\end{bmatrix} \tag{45}$$

where $\mathbf{Z}_n$, $\mathbf{U}_n$, and $\mathbf{N}_n$ are vectors of the received samples, of the transmitted symbols and of the noise samples, respectively, of the alien systems. The definitions of the block matrices C, C_n and T_n depend on both the channel and the characteristics of the alien DSL systems, and although T is block diagonal, this property will not generally hold for the other matrices.

In the case where $\mathbf{Z}$ and $\mathbf{Z}_n$ correspond to systems belonging to different service providers, it is currently very difficult to identify the crosstalk coupling matrices C and C_n. This occurs

because in the current unbundling framework there is no way for the first provider to obtain access to either $\mathbf{Z}_n$ or $\mathbf{U}_n$, and similarly for the second provider. However, the "third party" concept (see [36]) overcomes this difficulty by introducing an impartial third-party site, which captures all transmitted and received data, and is capable of producing estimates of the crosstalk coupling matrices.

With this in mind, the knowledge of C can be taken for granted, and a number of criteria can be devised to mitigate the effect of crosstalk into the alien systems. A possible solution would be to transmit in the null-space of C, thus causing theoretically zero crosstalk. Of course, this implies that some dimensions of $\mathbf{U}$ must be "sacrificed," so that transmission in the null-space is achieved. Although one could envisage scenarios where application of this method may be promising, this will not be further pursued here.

Limiting the FEXT in the mean square sense, results in the following conditions:

$$\sum_{k=1}^{L} \sum_{i \in \mathcal{N}_{\text{up}}} |c_{j,(k-1)N+i}|^2 \mathcal{E}^i_{k,\text{up}} \leq \mathcal{E}^c_{j,\text{up}}, \qquad j = 1, \ldots, MN_N \tag{46}$$

and

$$\sum_{k=1}^{L} \sum_{i \in \mathcal{N}_{\text{down}}} |c_{j,(k-1)N+i}|^2 \mathcal{E}^i_{k,\text{down}} \leq \mathcal{E}^c_{j,\text{down}}, \qquad j = 1, \ldots, MN_N \tag{47}$$

where M is the number of neighboring systems, N_N is the number of "dimensions" (e.g., number of tones) per neighboring system, $\mathcal{E}^c_{j,\text{up}}, \mathcal{E}^c_{j,\text{down}}$ are the maximum allowable crosstalk energies in sample j of the neighboring systems for upstream and downstream, and $c_{j,l}$ is the (j, l) element of the $MN_N \times LN$ matrix C. Note that this approach can be generalized, so that both FEXT and NEXT are restricted.

The set of inequalities in (46) and (47), combined correspondingly with those of (37) and (39), form a set of linear inequality constraints. Including the rate maximization objective of (33) yields the following optimization problems:

$$\max \quad \sum_{k=1}^{L} a_k \sum_{i \in \mathcal{N}_{\text{up}}} \frac{1}{2} \log_2 \left(1 + \frac{|r^i_{k,k}|^2 \mathcal{E}^i_{k,\text{up}}}{\Gamma} \right) \tag{48}$$

$$\text{subject to} \sum_{i \in \mathcal{N}_{\text{up}}} \mathcal{E}^i_{k,\text{up}} \leq \mathcal{E}_{k,\text{up}}, \qquad k = 1, \ldots, L \tag{49}$$

$$\sum_{k=1}^{L} \sum_{i \in \mathcal{N}_{\text{up}}} |c_{j,(k-1)N+i}|^2 \mathcal{E}^i_{k,\text{up}} \leq \mathcal{E}^c_{j,\text{up}}, \qquad j = 1, \ldots, MN_N \tag{50}$$

and

$$\max \quad \sum_{k=1}^{L} a_k \sum_{i \in \mathcal{N}_{\text{down}}} \tfrac{1}{2} \log_2 \left(1 + \frac{|r^i_{k,k}|^2 \mathcal{E}^i_{k,\text{down}}}{\Gamma} \right) \tag{51}$$

$$\text{subject to} \sum_{i \in \mathcal{N}_{\text{down}}} \mathcal{E}^i_{k,\text{down}} \leq \mathcal{E}_{k,\text{down}}, \qquad k = 1, \ldots, L \tag{52}$$

$$\sum_{k=1}^{L} \sum_{i \in \mathcal{N}_{\text{down}}} |c_{j,(k-1)N+i}|^2 \mathcal{E}^i_{k,\text{down}} \leq \mathcal{E}^c_{j,\text{down}}, \qquad j = 1, \ldots, MN_N. \tag{53}$$

The objective functions are concave (since they are sums of log functions), and the constraints form convex sets (because they are linear inequalities). Thus, solutions can be efficiently produced using convex programming techniques, and such an example is given in Section V-B. It is worth observing that other restrictions (such as PSD masks or bit caps) are easy to include in the above optimization problems, since they only require the introduction of linear inequality constraints, which preserve the convexity of the problem.

C. Energy Allocation and Upstream/Downstream Frequency Selection

Although all existing DSL systems employing FDD have a fixed upstream/downstream frequency duplexing band plan, there is evidence that a dynamically configured band plan offers significant advantages (see [37]). Such a plan is common for all users, but is determined during modem initialization, depending on the specific transmission environment, as well as on the user requirements. The disadvantages of a fixed band plan are exemplified in the presence of bridged taps, where transmission in one direction may face a disproportionate degradation, while transmission in the opposite direction may remain unscathed. On the other hand, adopting a dynamic plan in such a case enables a fairer distribution of the impact on both upstream and downstream. Additionally, a dynamic band plan gives extra flexibility by allowing the provisioning of either symmetric rates (in areas with several business customers) or asymmetric rates (in areas dominated by residential customers).

The optimization objective is now expressed by

$$\max \sum_{k=1}^{L} (a_{k,\text{up}} R_{k,\text{up}} + a_{k,\text{down}} R_{k,\text{down}}) \tag{54}$$

where $a_{k,\text{up}}, a_{k,\text{down}} \geq 0$ are the weights assigned to upstream and downstream transmission for user k, and $R_{k,\text{up}}, R_{k,\text{down}}$ are the achievable upstream and downstream rates of user k. Here, the optimization parameters involve not just the energies assigned but also the selection of upstream/downstream tones. However, if (34) and (35) are used, the partition of the set of tones into $\mathcal{N}_{\text{up}}$ and $\mathcal{N}_{\text{down}}$ is a binary constrained problem, whose solution has very high complexity.

Instead, the binary constraints can be relaxed, which greatly simplifies the computations. This idea has previously been exploited in [38] for subcarrier allocation in multiuser orthogonal-frequency-division-multiplexing, and in [39] for the computation of the FDMA capacity of the Gaussian multiple access channel in the presence of ISI. In more detail, it is initially

assumed that each tone is time-shared between upstream and downstream, thus obtaining the following achievable rates:

$$R_{k,\,\mathrm{up}} = \sum_{i=1}^{N} t_{i,\,\mathrm{up}}\,\frac{1}{2}\,\log_2\left(1+\frac{|r^i_{k,k}|^2\mathcal{E}^i_{k,\,\mathrm{up}}}{t_{i,up}\Gamma}\right) \tag{55}$$

$$R_{k,\,\mathrm{down}} = \sum_{i=1}^{N} t_{i,\,\mathrm{down}}\,\frac{1}{2}\,\log_2\left(1+\frac{|r^i_{k,k}|^2\mathcal{E}^i_{k,\,\mathrm{down}}}{t_{i,down}\Gamma}\right) \tag{56}$$

where $t_{i,\,\mathrm{up}}$, $t_{i,\,\mathrm{down}}$ describe the fraction of time in tone i used for upstream and downstream transmission correspondingly, and $t_{i,\,\mathrm{up}} + t_{i,\,\mathrm{down}} = 1$, $t_{i,\,\mathrm{up}}, t_{i,\,\mathrm{down}} \geq 0$. The existence of $t_{i,\,\mathrm{up}}$ and $t_{i,\,\mathrm{down}}$ in the denominators inside the log expressions implies that the assigned energy is "boosted," since transmission takes place over only some fraction of time. The energy constraints for user k are

$$\sum_{i=1}^{N} \mathcal{E}^i_{k,\,\mathrm{up}} \leq \mathcal{E}_{k,\,\mathrm{up}} \tag{57}$$

$$\sum_{i=1}^{N} \mathcal{E}^i_{k,\,\mathrm{down}} \leq \mathcal{E}_{k,\,\mathrm{down}}. \tag{58}$$

Therefore, the optimization problem has the following form:

$$\max \quad \sum_{k=1}^{L}\left[a_{k,\,\mathrm{up}}\sum_{i=1}^{N} t_{i,\,\mathrm{up}}\,\frac{1}{2}\,\log_2\left(1+\frac{|r^i_{k,k}|^2\mathcal{E}^i_{k,\,\mathrm{up}}}{t_{i,up}\Gamma}\right)\right.$$
$$\left. + a_{k,\,\mathrm{up}}\sum_{i=1}^{N} t_{i,\,\mathrm{down}}\,\frac{1}{2}\,\log_2\left(1+\frac{|r^i_{k,k}|^2\mathcal{E}^i_{k,\,\mathrm{down}}}{t_{i,down}\Gamma}\right)\right] \tag{59}$$

$$\text{subject to} \sum_{i=1}^{N} \mathcal{E}^i_{k,\,\mathrm{up}} \leq \mathcal{E}_{k,\,\mathrm{up}}, \qquad k = 1, \ldots, L \tag{60}$$

$$\sum_{i=1}^{N} \mathcal{E}^i_{k,\,\mathrm{down}} \leq \mathcal{E}_{k,\,\mathrm{down}}, \qquad k = 1, \ldots, L \tag{61}$$

$$t_{i,\,\mathrm{up}} + t_{i,\,\mathrm{down}} = 1, \qquad i = 1, \ldots, N. \tag{62}$$

The objective function is concave, because it is a sum of functions of the form $x\log(1+y/x)$, which are shown to be convex in $x,\ y \geq 0$ in [39]. The constraint sets are clearly convex, since they are defined by linear inequalities. Therefore, the problem is convex and a variety of methods can be used to efficiently derive a solution.

Still, such a solution would actually yield a hybrid between an FDD and a time-division duplexing (TDD) implementation. Since an FDD implementation is required, an approximate such solution is obtained by rounding $t_{i,\,\mathrm{up}}$ and $t_{i,\,\mathrm{down}}$. Naturally, this is suboptimal, but when the number of tones is fairly large, it will be adequately close to the optimal solution. Simulation results in Section V-C validate this claim. Note that the power-backoff constraints of the previous subsection can also be included in the problem formulation without considerably affecting the difficulty of obtaining a solution.

TABLE I
SIMULATION PARAMETERS

Number of DMT Tones	4096
Tone Width	4.3125 KHz
Symbol Rate	4 KHz
Coding Gain	3.5 dB
Noise Margin	6 dB
Symbol Error Probability	$< 10^{-7}$
Maximum Power	14.5 dBmW
Cable Type	26-Gauge (0.4 mm)
Source/Load Resistance	100 Ohm
Amateur Radio Bands	as specified in [1]

In all the previous problems, the objective has been the maximization of a weighted data rate sum. It should be evident that by adjusting the weights, one obtains different surface points of the data rate region achievable by vectored transmission, and thus the whole multidimensional surface can be traced. However, visualizing the inherent tradeoffs becomes difficult when the weighted sums include more than three terms. The practical question, which will likely be posed to a service provider, is whether the vectored system can support a set of rate requirements, and if so, what is the energy allocation achieving the requirements. Appendix II shows that this problem actually has a duality relationship with the weighted data rate sum problem, and thus the weighted sum problem provides an alternative method to solve the "feasibility" problem.

V. SIMULATION RESULTS

The simulation results presented next refer to the VDSL environment. The general parameters and the DMT specifications (shown in Table I) are from [1], [4], and [3], [5], correspondingly. The specified coding gain, noise margin, and probability of error target lead to a transmission gap of 12 dB. In the following, infinite granularity for the number of bits on each tone is assumed, and error propagation effects in upstream are ignored. Deliberately, no bit cap was taken into account, since the purpose of the simulations is to demonstrate the achievable upper bounds.

A. Results for Energy Allocation Optimization and Channel Estimation Errors

The energy allocation method of Section IV-A amounts to performing water filling independently for each user. The upstream/downstream frequency division is chosen as shown in Table II, and the noise models used are specified in [40]. A "uniform" loop topology with 20 users is assumed, meaning that all loops have the same length. Figs. 15 and 16 compare the achievable data rates of "conventional" DMT and vectored-DMT versus the loop length with either noise A or noise F, for upstream and downstream transmission, respectively. Although no PSD constraint was enforced, the resulting PSDs

TABLE II
UPSTREAM–DOWNSTREAM FREQUENCY ASSIGNMENT

Upstream Bands (MHz)	Downstream Bands (MHz)
$0.03 - 0.138$	$0.138 - 2.5$
$2.5 - 3.75$	$3.75 - 7.5$
$7.5 - 14.5$	$14.5 - 17.7$

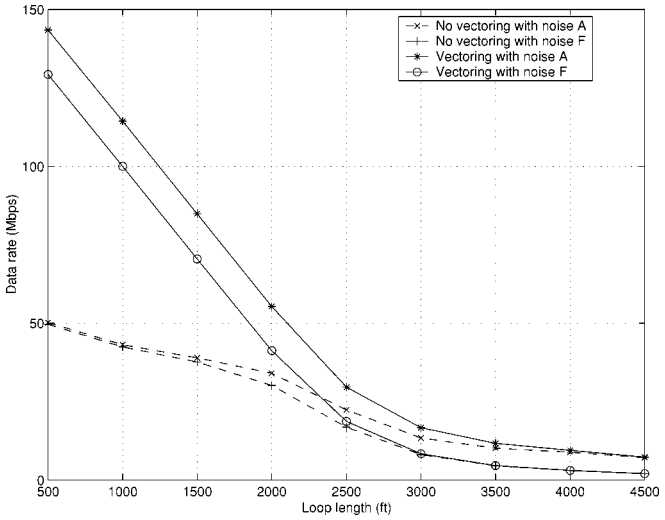

Fig. 15. Upstream VDSL data rates.

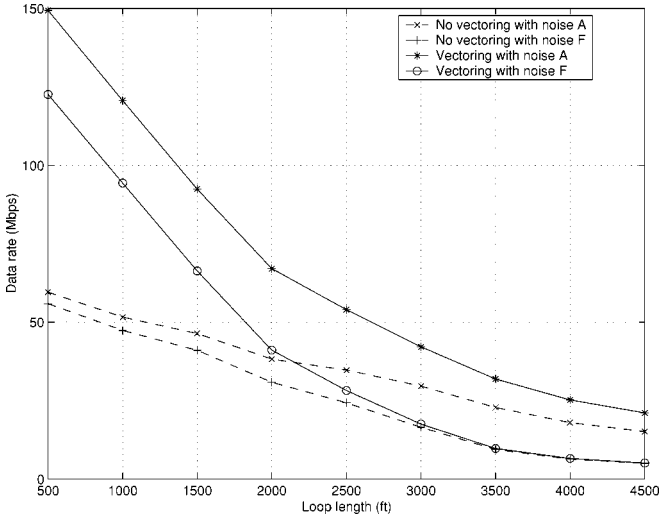

Fig. 16. Downstream VDSL data rates.

were observed to be typically below -52 dBmW/Hz, and the peak never exceeded the value of -45 dBmW/Hz.

Evidently, vectoring improves performance significantly, and this can be viewed in two ways. For a given loop length, VDMT allows the achievement of much higher data rates. The rate increases are considerable for lengths shorter than 4500 ft in noise A, or 3500 ft in noise F. The gains become spectacular in short loops, where obviously transmission is FEXT-limited. Also, it is seen that VDMT extends the maximum loop length given a

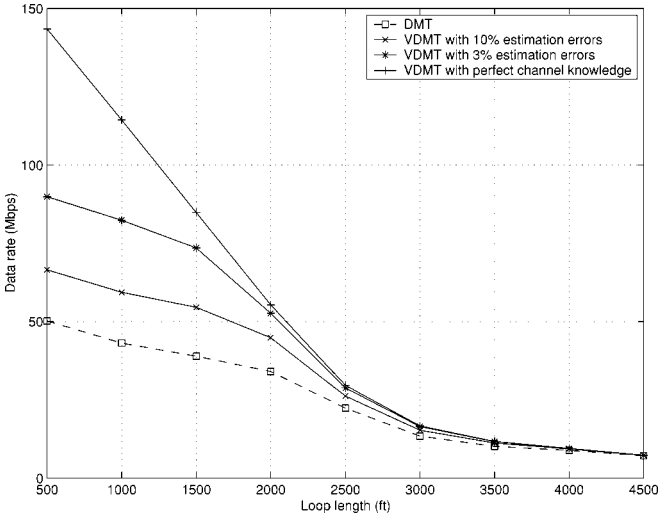

Fig. 17. Upstream VDSL data rates (noise A) with channel estimation errors.

data rate requirement. As an example, in Fig. 16, a downstream rate requirement of 50 Mbps limits DMT systems with noise of type A to loops shorter than 1150 ft, while employing VDMT extends the reach to 2650 ft. Simulations not shown here indicate that including a bit cap of 11 bits per tone has noticeable effects only in loops shorter than 1500 ft, where upstream rates are restricted to 80 Mbps, while downstream rates are restricted to 90 Mbps.

Next, the impact of channel estimation errors in a worst-case scenario is assessed. Equations (31) and (32) indicate that the effects of such errors are residual crosstalk, which may be treated as noise, and detection biasing, which can be modeled as a decrease in the minimum distance of the constellation points (e.g., see [41]). Here, the effect of residual crosstalk is examined, and simulation results are shown, where the energy allocation algorithm accounts for estimation errors by considering them as extra noise. By making the approximations $Q_i \approx I$ and that E_i has zero diagonal elements, the covariance matrix of the extra noise term in tone i is $[\mathrm{diag}(\hat{R}_i)]^{-1} E_i E(\mathbf{U}_i \mathbf{U}_i^*)\ E_i [\mathrm{diag}(\hat{R}_i)]^{-*}$ for upstream, and $[\mathrm{diag}(\hat{R}_i^T)]^{-1} E_i^T E(\mathbf{U}_i' \mathbf{U}_i'^*)\ E_i^{T*} [\mathrm{diag}(\hat{R}_i^T)]^{-*}$ for downstream. Assuming a worst case situation, E_i has all its off-diagonal elements equal to ε and the variance of $\mathbf{U}_i$ and $\mathbf{U}_i'$ is σ_u^2. With the additional approximation of uncorrelated components of $\mathbf{U}_i'$, it is found that the energy of the noise contribution due to channel estimation errors in tone i for user k is

$$\sigma_{i,k}^2 = (L-1)|r_{k,k}^i|^{-2}|\varepsilon|^2\sigma_u^2 \tag{63}$$

holding for both upstream and downstream transmission.

Making the pessimistic assumption that $\sigma_u^2 = -50$ dBm, Figs. 17 and 18 show the impact of channel estimation errors on the achievable upstream and downstream data rates for the noise A environment. The curves are parameterized by the *relative* estimation error $|\varepsilon|/|r_{k,k}^i|$, and it is seen that as channel identification becomes less accurate, vectored-DMT performance diminishes to that of DMT.

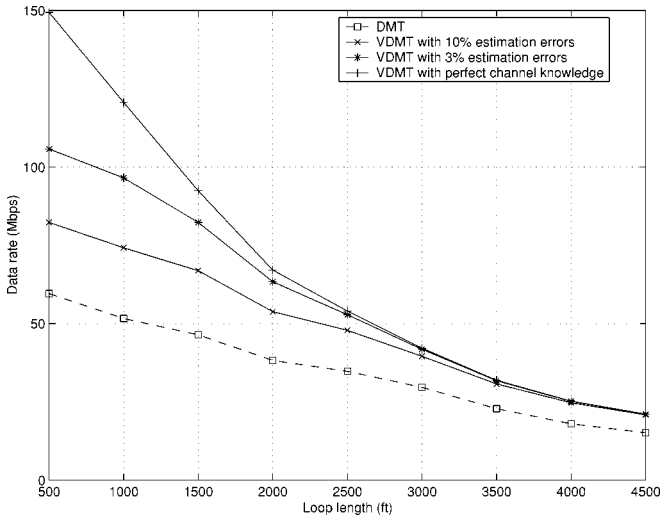

Fig. 18. Downstream VDSL data rates (noise A) with channel estimation errors.

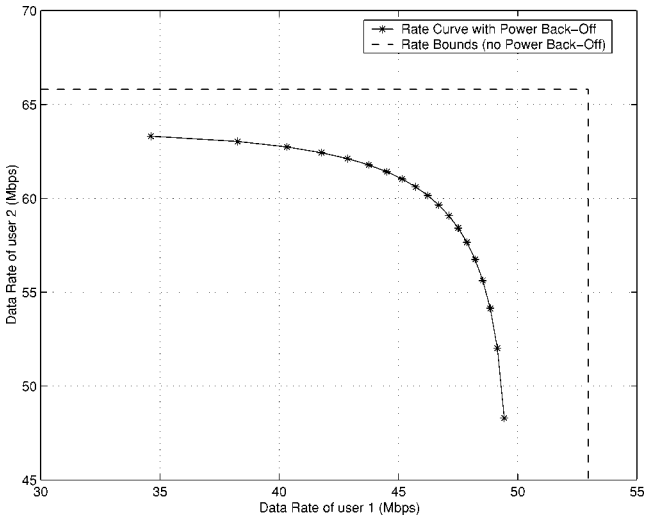

Fig. 19. Rate region for two users with power backoff.

B. Example of Energy Allocation With Power Backoff Optimization

Next, an example is given where energy allocation is further constrained by the requirement that some "alien" DSL system must also be protected against crosstalk from the vectored system. Assume that there are two vectored users and a single affected CO-based system as in Fig. 14, where obviously downstream transmission from the CO is severely impaired. The loop lengths of the vectored users are 2500 ft and 2000 ft, the loop length of the affected user is 3000 ft, and the crosstalk coupling length between the vectored and the alien system is 1500 ft.

Assuming the existence of a VDSL system on the affected line, a possible strategy to mitigate the impact of crosstalk is to postulate that the induced crosstalk must not exceed the crosstalk PSD caused by a certain number of VDSL disturbers with loop lengths equal to the length of the affected line (this is analogous to the power backoff method of [42]). Employing the well-known T1E1.4 FEXT model, (47) must then be satisfied with

$$\mathcal{E}^{c}_{j,\,\mathrm{down}} = PSD(f_j) k_{\mathrm{FEXT}} l f_j^2 |H(f_j)|^2 \left(\frac{N_d}{49}\right)^{0.6} \qquad j = 1, \ldots, N \tag{64}$$

where f_j is the center frequency of tone j, $H(f)$ and l are the transfer function and the length of the affected line (in feet), $PSD(f)$ is the VDSL PSD mask, N_d is the number of disturbers, and k_{FEXT} is a constant equal to $7.999 \cdot 10^{-20}$. In the following, the coefficients $c_{j,l}$ of (47) were computed by making the approximation that signals transmitted in a tone do not cause crosstalk in neighboring tones, and N_d was chosen to be 20.

Fig. 19 shows the achievable downstream rate curve, where the different points are obtained by adjusting the weights in (33). The nonlinear programming package MINOS (see [43]) is used, with all transmission parameters set as before, assuming noise of type A. The dashed curve indicates the achievable rate bounds in the absence of crosstalk constraints. The practical use of this result is that a service provider may perform power-backoff in a "selective" way, so that the performance impact can be distributed according to the service priorities.

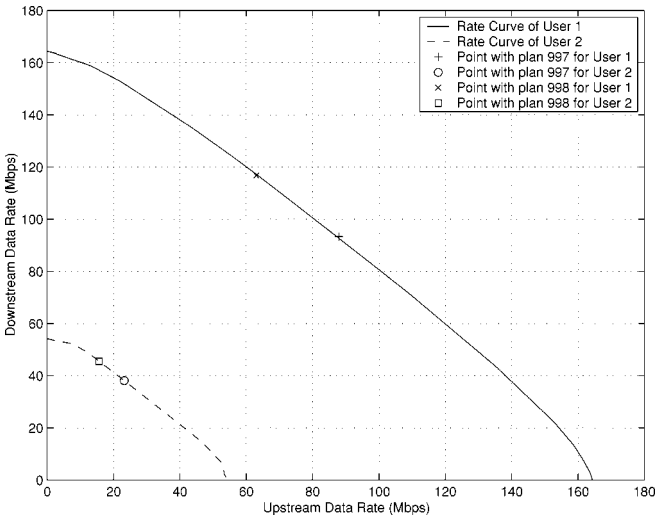

Fig. 20. Upstream/downstream rate regions for two users with optimum frequency duplexing.

C. Example of Joint Energy Allocation and Frequency Planning

Finally, it is assumed that the frequency plan for upstream/downstream duplexing is allowed to vary in each vectored bundle depending on the loop characteristics and the service requirements. Results for two users are shown, where user 1 and user 2 have loop lengths of 1500 and 3000 ft, correspondingly. Noise A is considered, and all transmission parameters are the same as before, with the difference being that the radio bands are now ignored and the number of tones is set to 128 in order to reduce the computational burden. The MINOS package is again used.

By having $\alpha_{1,\,\mathrm{up}} = \alpha_{2,\,\mathrm{up}}$, $\alpha_{1,\,\mathrm{down}} = \alpha_{2,\,\mathrm{down}}$, and adjusting the upstream/downstream weights, the rate curves of Fig. 20 are produced. The rates achieved with the currently

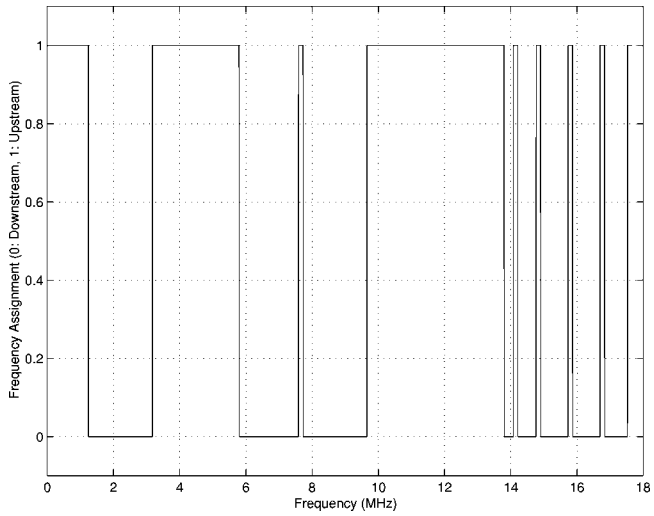

Fig. 21. Optimum frequency duplexing plan with symmetric service for upstream and downstream.

proposed VDSL band plans 997 and 998 (see [44]) are also shown. The optimal frequency allocation for almost symmetric transmission is shown in Fig. 21. The corresponding achievable rates are $R_{1,\,\mathrm{up}}$ =89.7 Mbps, $R_{1,\,\mathrm{down}} = 90.8$, $R_{2,\,\mathrm{up}} =$ 32.0 Mbps, and $R_{2,\,\mathrm{down}} = 29.3$ Mbps, which are obtained with $\alpha_{1,\,\mathrm{up}} = \alpha_{2,\,\mathrm{up}} = 0.4998$.

VI. Comparison With Information Theory Results

In this section, the proposed crosstalk removal techniques are compared against information theoretic bounds, and it is demonstrated that the techniques are capable of achieving rates very close to the optimum.

Starting with the vector channel of (3), and assuming a total energy constraint, it is known that the single-user capacity equals:

$$C^{SU} = \max_{R_{\mathbf{xx}}} \tfrac{1}{2} \log|HR_{\mathbf{xx}}H^* + I| \quad \text{subject to trace } (R_{\mathbf{xx}}) \le \mathcal{E} \tag{65}$$

where $R_{\mathbf{xx}}$ is the input covariance matrix, and $\mathcal{E}$ is the maximum total energy. The optimum $R_{\mathbf{xx}}$ is such that its eigenvectors are equal to the right singular vectors of H, and its eigenvalues are obtained by water filling across the singular values of H [45]. However, achieving this capacity requires *coordination* both at the transmitter and at the receiver side. Clearly, this is not the case for DSL, where coordination is only possible at one side, and multiple users exist. Still, it will be shown that (65) serves as a useful bound on the achievable DSL performance.

Examining Fig. 3, one observes that *upstream* communication corresponds to the case of transmission in a *vector Gaussian multiple access channel*. Similarly, *downstream* communication corresponds to the *vector Gaussian broadcast channel*. In the following, some results regarding the capacity region of these channels are reviewed, and bounds are expressed for the corresponding regions.

For the vector multiple access channel, coordination is possible only among the receivers. Also, individual energy constraints apply to each user. Let $H = [H_1 H_2 \cdots H_L]$, where H_i is comprised of those columns of H corresponding to $\mathbf{x}_i$. The capacity region is then described as (see [46] and [47]) (66) shown at the bottom of the page, where $\mathcal{E}_i$ is the total energy allowed for user i. An illustration of the capacity region for two users is given in Fig. 22, and it is seen that the region is defined as the union of pentagons corresponding to all possible input covariance matrices. In that case, the capacity region is a subset of the following region:

$$\mathcal{C}^{MAC-UB} = \left[(R_1, \ldots, R_L): \begin{cases} R_i \le \max_{\mathrm{trace}(R_{\mathbf{x_i x_i}}) \le \mathcal{E}_i} \\ \quad \tfrac{1}{2} \log|H_i R_{\mathbf{x_i x_i}} H_i^* + I|, \\ \quad i = 1, \ldots, L \\ \sum_{i=1}^{L} R_i \\ \quad \le \max_{\mathrm{trace}(R_{\mathbf{xx}}) \le \sum_{i=1}^{L} \mathcal{E}_i} \\ \quad \tfrac{1}{2} \log|HR_{\mathbf{xx}}H^* + I| \end{cases} \right] \tag{67}$$

which corresponds to the upper bounds obtained by assuming that there is only one user transmitting, or that coordination is possible among the transmitters.

For the vector broadcast channel, coordination is possible only among the transmitters, where the transmitter output is characterized by a total energy constraint. The capacity region remains unsolved except in the special case of the *degraded* broadcast channel. Still, a few results exist with regard to the sum capacity.

Reference [48] proposed (independently of this work) the use of the QR decomposition to form a set of interference channels, where the interference is noncausally known to the transmitters. Then, *lattice precoding* (see [49]) was adopted, thus achieving complete removal of the interference without any transmission energy increase. This scheme is named *Ranked Known Interference* and was proved to be asymptotically sum capacity optimal both for low and high SNR. Lattice precoding is a generalization of the *modulo precoding* proposed in this paper. It is later shown that for DSL channels, the performance difference between the two schemes is very small, although the complexity of lattice precoding is significantly higher. Another recent piece of work [50] expresses the solution for the sum capacity as the result of a *game*, with a "signal player" choosing a transmission covariance matrix to maximize the sum rate, and a "noise player" choosing a noise covariance matrix to minimize the sum rate.

$$\mathcal{C}^{MAC} = \bigcup_{R_{\mathbf{x_1 x_1}}, \ldots, R_{\mathbf{x_L x_L}}} \left[(R_1, \ldots, R_L): \sum_{i \in S} R_i \le \tfrac{1}{2} \log \left| \sum_{i \in S} H_i R_{\mathbf{x_i x_i}} H_i^* + I \right|, \forall S \subseteq 1, \ldots, L \right]$$
$$\text{subject to trace } (R_{\mathbf{x_i x_i}}) \le \mathcal{E}_i, \quad i = 1, \ldots, L \tag{66}$$

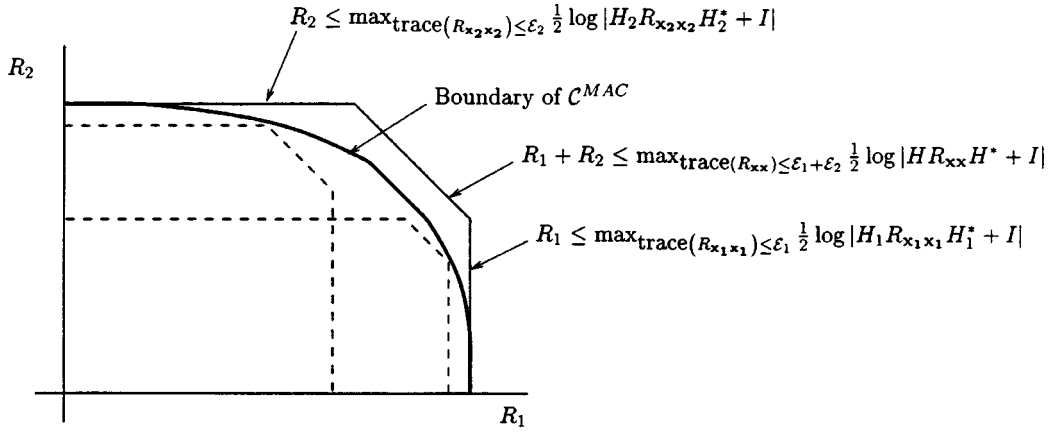

Fig. 22. Capacity region of the vector multiple access channel with two users.

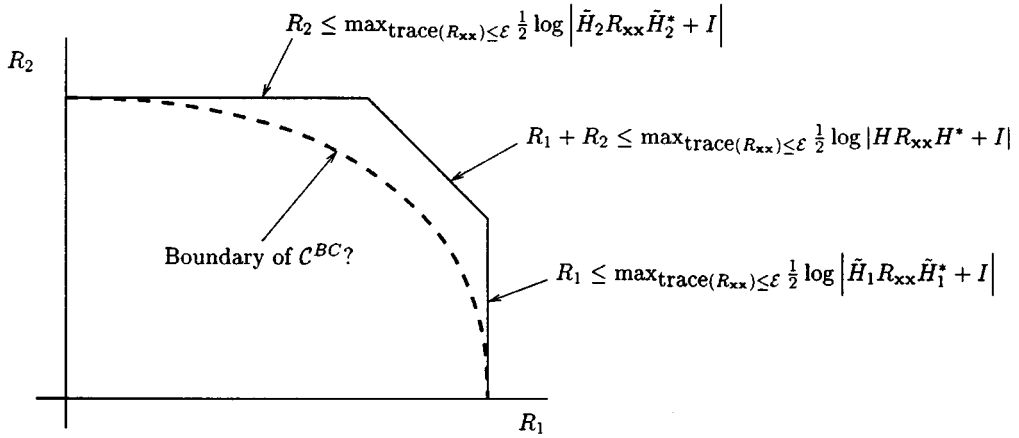

Fig. 23. Capacity region of the vector broadcast channel with two users.

Although the capacity region is unknown, it is a subset of the following region:

$$\mathcal{C}^{BC-UB} = \left[(R_1, \ldots, R_L): \begin{cases} R_i \le \max_{\text{trace}(R_{\mathbf{xx}})\le\mathcal{E}} \\ \quad \frac{1}{2}\log\left|\tilde{H}_i R_{\mathbf{xx}} \tilde{H}_i^* + I\right|, \\ \quad i = 1, \ldots, L \\ \sum_{i=1}^{L} R_i \\ \quad \le \max_{\text{trace}(R_{\mathbf{xx}})\le\mathcal{E}} \\ \quad \frac{1}{2}\log|H R_{\mathbf{xx}} H^* + I| \end{cases} \right] \quad (68)$$

where $\mathcal{E}$ is the total transmitter output energy, $H = [\tilde{H}_1^T \tilde{H}_2^T \cdots \tilde{H}_L^T]^T$, and $\tilde{H}_i$ is comprised of those rows of H corresponding to $\mathbf{y}_i$. The bounds defining this region are obtained by assuming that there is only one user receiving, or that coordination is possible among the receivers. An illustration for two users is shown in Fig. 23

The bounds defined by (67) and (68) are easy to compute, since they express single user capacities. Therefore, the rates obtained from these bounds can easily be compared against those of the proposed crosstalk mitigation techniques in a realistic DSL scenario. It is next assumed that there are only two users, where loop 1 is 1500 ft long and loop 2 is 2000 ft long. The other

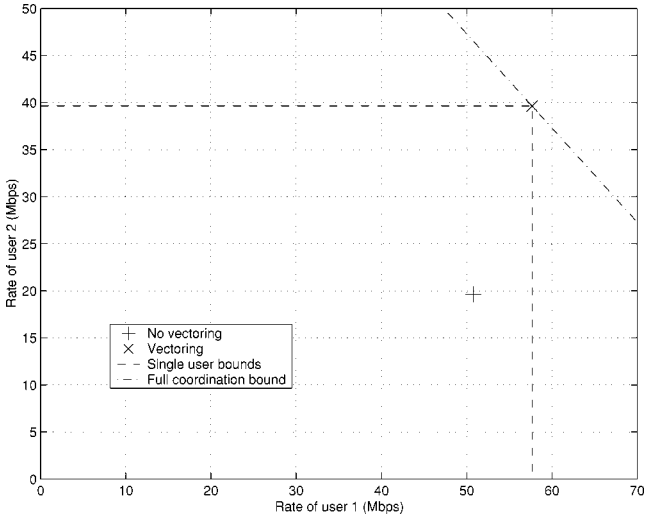

Fig. 24. Comparison of upstream rate regions.

simulation assumptions are identical to those of Section V. Note that the resulting SNR gap of 12 dB applies for all computed quantities, including the bounds.

Fig. 24 shows the upstream rate regions and theoretical bounds. As expected, the rate improvement from vectoring is significant especially for user 2. But even more interestingly, the rates achieved with vectoring almost coincide with the

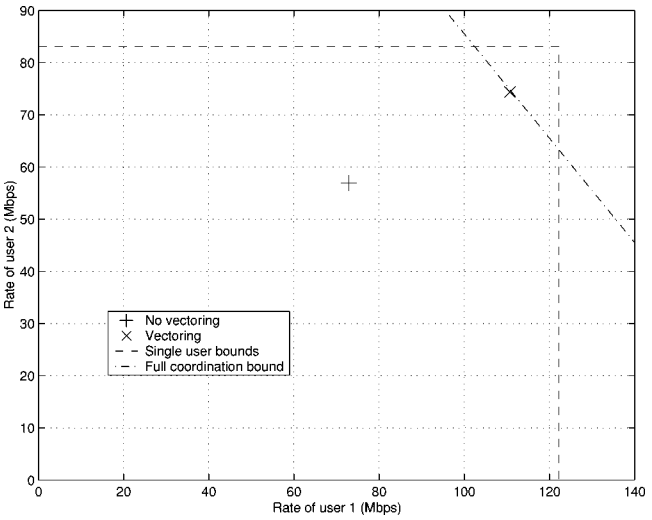

Fig. 25. Comparison of downstream rate regions.

single user and full coordination bounds of the multiple access channel. Fig. 25 shows the corresponding downstream rate regions and theoretical bounds. Again, the rate increase from vectoring is quite large, and additionally, the sum rate is very close to the bound obtained from full coordination. The user rates are rather smaller than the single user bounds, but that can be justified by the fact that, in vectoring, individual energy contraints apply for each user, whereas (68) employs a total energy constraint.

The above results testify that the room for improvement by adopting more advanced methods (e.g., lattice instead of modulo precoding, or MMSE criterion for crosstalk cancellation) is rather small. Also, it can be claimed that, in DSL channels, coordination at one side (such as in vectoring) performs with regard to the sum rate almost as well as full coordination. This is the consequence of the special property of DSL channels, where within each tone, the upstream channel matrix is *column-wise diagonally dominant*, while the downstream channel matrix is *row-wise diagonally dominant*.

VII. Conclusion

This paper presented the concept of vectored transmission applied to DSL systems. The method can be summarized as employing joint signal processing techniques at the CO/ONU site, thus taking advantage of user coordination to mitigate crosstalk. Structures were presented, where crosstalk is removed individually in each tone, and it was demonstrated that these perform very close to perfect crosstalk cancellation. Furthermore, adopting transmission optimization techniques allowed extra performance benefits, while at the same time transmission constraints (such as emission restrictions) were taken into account. In these cases, weighted data rate sum maximization criteria were used. Additionally, the performance of vectored transmission was shown to be very close to bounds obtained from information theory.

The implementation of vectored systems holds the promise to greatly improve DSL systems, offering advantages to both customers and service providers. At the cost of synchronization of all users, channel matrix identification, and extra signal processing at the CO/ONU, considerable data rate increases can be achieved for both upstream and downstream transmission. Universal PSD mask constraints can be replaced by flexible power backoff strategies adaptable to the specific crosstalk environment. Additionally, fixed frequency duplexing plans can be substituted by dynamically determined plans tailored to the specific channel and user requirements. In conclusion, service providers are given the freedom to define different classes of service and to allocate the available resources according to the requirements of each class.

Appendix I
Bounds for the QR Decomposition

This appendix derives bounds for the diagonal elements of the upper triangular matrix R obtained from the QR decomposition of a DSL channel matrix T corresponding to a specific tone. The case of an upstream channel is examined, however, the results are easily extended to downstream by taking into account the reciprocity property for twisted pair transmission. For the purpose of geometric illustration, the proofs assume real matrices, but the derived bounds also hold for complex matrices.

Letting $\mathbf{t}_j$ be the jth column of T, and t_{ij} be the (i, j) element of T, the condition of "column-wise" dominant diagonal elements may be expressed as

$$|t_{ij}| \leq |t_{jj}| \tan\alpha, \qquad i \neq j \tag{69}$$

where $0 \leq \alpha \leq \pi/2$ has the geometric interpretation of being the maximum angle between axis j and the projection of vector $\mathbf{t}_j$ on the (i, j) plane. For *any* DSL upstream channel matrix T, α is very small (see Fig. 10).

The aim is to derive bounds for $|r_{jj}|$ (the magnitude of the diagonal elements of R) with respect to $|t_{jj}|$ (the magnitude of the diagonal elements of T). Starting with $|r_{11}|$, one observes that

$$\begin{aligned} |r_{11}| &= |\mathbf{t}_1| = \sqrt{\sum_{i=1}^{L} |t_{i1}|^2} \\ &\leq |t_{11}| \sqrt{1 + (L-1)\tan^2\alpha} \qquad (70) \\ &\leq |t_{11}| \left[1 + (L-1)\frac{\tan^2\alpha}{2}\right] \qquad (71) \end{aligned}$$

where (70) makes use of (69), and (71) results from $\sqrt{1+x} \leq 1 + x/2$. The following obvious lower bound can also be obtained

$$|r_{11}| \geq |t_{11}|. \tag{72}$$

Next, bounds are obtained for $|r_{22}|$. The examination of Fig. 27 reveals that the upper bound on $|r_{22}|$ is achieved when $\mathbf{t}_1 \perp \mathbf{t}_2$, in which case $r_{12} = 0$ and

$$\begin{aligned} |r_{22}| &= |\mathbf{t}_2| \\ &\leq |t_{22}| \left[1 + (L-1)\frac{\tan^2\alpha}{2}\right]. \qquad (73) \end{aligned}$$

For the lower bound, letting $t_{2i} = 0$ for $i \neq 1, 2$ suffers no loss of generality. Then, $|r_{22}|$ is minimized, when the angle between

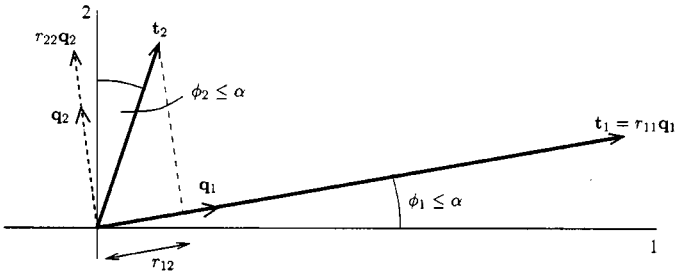

Fig. 26. Illustration for QR bounds derivation.

$\mathbf{q}_1$ and $\mathbf{t}_2$ is minimized. As shown in Fig. 26, this occurs when the angle equals $\pi/2 - 2\alpha$, in which case

$$|r_{12}| = |\mathbf{t}_2| \cos(\pi/2 - 2\alpha) = |\mathbf{t}_2| \sin 2\alpha. \tag{74}$$

Therefore

$$|r_{22}| = \sqrt{|\mathbf{t}_2|^2 + |r_{12}|^2 - 2|\mathbf{t}_2||r_{12}| \sin 2\alpha} \tag{75}$$

$$\geq \sqrt{|\mathbf{t}_2|^2 + |\mathbf{t}_2|^2 \sin^2 2\alpha - 2|\mathbf{t}_2|^2 \sin 2\alpha \sin 2\alpha} \tag{76}$$

$$= |\mathbf{t}_2| \sqrt{1 - \sin^2 2\alpha}$$

$$\geq |t_{22}| \sqrt{1 - \sin^2 2\alpha} \tag{77}$$

$$\geq |t_{22}| \sqrt{1 - 4\alpha^2} \tag{78}$$

where (75) results from vector addition, (76) makes use of (74), (77) uses the fact $|\mathbf{t}_2| \geq |t_{22}|$, and (78) results from $\sin(x) \leq x$.

Similar arguments that were used for deriving the bounds of $|r_{22}|$ can be used for $|r_{jj}|$. The upper bound on $|r_{jj}|$ is achieved when $\mathbf{t}_j \perp \mathbf{t}_k$, $k < j$, in which case

$$|r_{jj}| = |\mathbf{t}_j| \leq |t_{jj}| \left[1 + (L-1) \frac{\tan^2 \alpha}{2}\right]. \tag{79}$$

For the lower bound, it is seen that $|r_{jj}|$ is minimized, when the angle between $\mathbf{q}_{j-1}$ and $\mathbf{t}_j$ is minimized. Again, this angle must be greater than $\pi/2 - 2\alpha$, which leads to

$$|r_{jj}| \geq |t_{jj}| \sqrt{1 - 4\alpha^2}. \tag{80}$$

In conclusion, the following bounds hold for all j:

$$|t_{jj}| \sqrt{1 - 4\alpha^2} \leq |r_{jj}| \leq |t_{jj}| \left[1 + (L-1) \frac{\tan^2 \alpha}{2}\right]. \tag{81}$$

Evidently, for a sufficiently small α, it is practical to assume that $|r_{jj}| \simeq |t_{jj}|$. This condition holds for *all* realistic DSL channels.

In general, exchanging the columns of a matrix has a significant effect on its QR decomposition. (This corresponds to a right multiplication of the matrix with a permutation matrix.) However, for the channel matrices encountered in DSL and making use of the above result, it is easy to notice that the impact of this operation is hardly noticeable.

Appendix II
Duality Between the Feasibility Problem and the Weighted Data Rate Sum Maximization Problem

The rate feasibility problem is expressed by the following requirements:

$$R_k(\mathbf{E}) \geq r_k, \qquad k = 1, \ldots, L \tag{82}$$

where r_k is the rate requirement, $R_k(\mathbf{E})$ is the rate of user k, and $\mathbf{E}$ represents the energy allocation. Here, the requirements refer to either upstream or downstream, but (82) (as well as the conclusions that follow) can be extended to a joint downstream/upstream feasibility problem. Additionally, the domain of $\mathbf{E}$ is defined, such that the relevant energy constraints [for instance those of (37), (39), (46), or (47)] are satisfied.

The functions $R_k(\mathbf{E})$ are concave in $\mathbf{E}$, since their domains are convex sets, and they are defined as sums of log functions. Thus, the feasibility problem may be posed as the following convex problem:

$$\min \qquad 0 \tag{83}$$

$$\text{subject to } -R_k(\mathbf{E}) + r_k \leq 0, \qquad k = 1, \ldots, L \tag{84}$$

where any feasible solution is actually acceptable. Reference [51] describes the so-called Phase-I method, which can be employed here to provide a solution. An alternative formulation is

$$\min \qquad -R_L(\mathbf{E}) + r_L \tag{85}$$

$$\text{subject to } -R_k(\mathbf{E}) + r_k \leq 0, \qquad k = 1, \ldots, L-1. \tag{86}$$

Here, the problem is feasible, if and only if the optimal value is found to be smaller or equal to zero. Interior point methods may be applied, where the algorithm may terminate as soon as some value smaller or equal to zero is achieved. In that case, the problem is declared feasible and the corresponding $\mathbf{E}$ is produced. If the optimum value is found to be larger than zero, then the problem is declared infeasible.

Forming the Lagrangian gives

$$L(\mathbf{E}, a_1, a_2, \ldots, a_L) = \sum_{k=1}^{L-1} a_k \left(-R_k(\mathbf{E}) + r_k\right) - R_L(\mathbf{E}) + r_L \tag{87}$$

and the dual function is

$$g(a_1, a_2, \ldots, a_L) = \min_{\mathbf{E}} L(\mathbf{E}, a_1, a_2, \ldots, a_L)$$

$$= \sum_{k=1}^{L-1} a_k r_k + r_L - \max_{\mathbf{E}} \left[\sum_{k=1}^{L-1} a_k R_k(\mathbf{E}) + R_L(\mathbf{E})\right]. \tag{88}$$

The function $g(a_1, a_2, \ldots, a_L)$ is concave as the minimum of a set of affine functions. The dual problem then is

$$\max_{a_1, a_2, \ldots, a_L} g(a_1, a_2, \ldots, a_L) = \tag{89}$$

$$\max_{a_1, a_2, \ldots, a_L} \left[\sum_{k=1}^{L-1} a_k r_k + r_L - \max_{\mathbf{E}} \cdot \left[\sum_{k=1}^{L-1} a_k R_k(\mathbf{E}) + R_L(\mathbf{E})\right]\right] \tag{90}$$

where $a_k \geq 0$, $k = 1, \ldots, L$. In the above, the weighted data rate sum maximization problem appears as a subproblem.

Let d^* be the optimal value of (90) and p^* be the optimal value of (85). Slater's condition (see [51]) states that if (86) are strictly feasible (i.e., there exists an $\mathbf{E}$, such that $-R_k(\mathbf{E}) + r_k < 0$ for $k = 1, \ldots, L-1$), then $d^* = p^*$. Therefore, solving the dual problem provides an alternative way to answer

the feasibility question. Again, interior point methods may be employed, which may terminate as soon as a positive value is achieved, and in which case the problem is declared infeasible. On the other hand, if the optimal value is found to be negative, then the problem is declared feasible and the corresponding $\mathbf{E}$ is produced.

ACKNOWLEDGMENT

The authors wish to thank the anonymous reviewers for suggesting the inclusion of information theoretic results and for several other comments that improved the paper considerably.

REFERENCES

[1] Q. Wang, Ed., Very-high-speed digital subscriber lines (VDSL) metallic interface, Part 1: Functional requirements and common specification. T1E1.4 Contribution 2000-009R3. [Online]. Available: http://www.t1.org/

[2] V. Oksman, Ed., Very-high-speed digital subscriber lines (VDSL) metallic interface, Part 2: Technical specification of a single-carrier modulation (SCM) transceiver. T1E1.4 Contribution 2000-011R3. [Online]. Available: http://www.t1.org/

[3] S. Schelstraete, Ed., Very-high-speed digital subscriber lines (VDSL) metallic interface, Part 3: Technical specification of a multicarrier modulation transceiver. T1E1.4 Contribution 2000-013R4. [Online]. Available: [Online]. Available: http://www.t1.org/

[4] Transmission and multiplexing (TM); Access transmission systems on metallic access cables; Very high speed digital subscriber line (VDSL); Part 1: Functional requirements. ETSI Doc. Nb. TS 101 270-1, Ver. 1.2.1. [Online]. Available: http://www.etsi.org/

[5] Transmission and multiplexing (TM); Access transmission systems on metallic access cables; Very high speed digital subscriber line (VDSL); Part 2: Transceiver specification. ETSI Doc. Nb. TS 101 270-2, Ver. 1.1.1. [Online]. Available: http://www.etsi.org/

[6] T. Starr, J. M. Cioffi, and P. J. Silverman, "Twisted pair transmission," in *Understanding Digital Subscriber Line Technology*. Englewood Cliffs, NJ: Prentice Hall, 1999, ch. 3.

[7] *Spectrum Management for Loop Transmission Systems*, ANSI standard, T1.417-2001, committee T1E1, Jan. 2001.

[8] J. M. Cioffi. (2001, Feb.) Unbundled DSL evolution. T1E1.4 Contribution 2001-088, Los Angeles, CA. [Online]. Available: http://www.t1.org/

[9] M. L. Honig, K. Steiglitz, and B. Gopinath, "Multichannel signal processing for data communications in the presence of crosstalk," *IEEE Trans. Commun.*, pt. 4, vol. 38, pp. 551–558, Apr. 1990.

[10] M. L. Honig, P. Crespo, and K. Steiglitz, "Suppression of near- and far-end crosstalk by linear pre- and post-filtering," *IEEE J. Select. Areas Commun.*, vol. 10, pp. 614–629, Apr. 1992.

[11] G. Tauböck and W. Henkel, "MIMO systems in the subscriber-line network," in *Proc. 5th Int. OFDM Workshop*, Hamburg, Germany, Sept. 2000, pp. 18.1–18.3.

[12] G. G. Raleigh and J. M. Cioffi, "Spatio–temporal coding for wireless communication," *IEEE Trans. Commun.*, vol. 46, pp. 357–366, Mar. 1998.

[13] G. D. Golden, J. E. Mazo, and J. Salz, "Transmitter design for data transmission in the presence of a data-like interferer," *IEEE Trans. Commun.*, pt. 2/3/4, vol. 43, pp. 837–850, Feb./Mar./Apr. 1995.

[14] P. S. Kumar and S. Roy, "Optimization for crosstalk suppression with noncoordinating users," *IEEE Trans. Commun.*, vol. 44, pp. 894–905, July 1996.

[15] M. Abdulrahman and D. D. Falconer, "Cyclostationary crosstalk suppression by decision feedback equalization on digital subscriber loops," *IEEE J. Select. Areas Commun.*, vol. 10, pp. 640–649, Apr. 1992.

[16] A. Peled and A. Ruiz, "Frequency domain data transmission using reduced computational complexity algorithms," in *Proc. IEEE ICASSP*, Denver, CO, Apr. 1980, pp. 964–967.

[17] F. Sjöberg, M. Isaksson, R. Nilson, P. Ödling, S. K. Wilson, and P. O. Börjesson, "Zipper: A duplex method for VDSL based on DMT," *IEEE Trans. Commun.*, vol. 47, pp. 1245–1252, Aug. 1999.

[18] F. Sjöberg, R. Nilson, M. Isaksson, P. Ödling, and P. O. Börjesson, "Asynchronous zipper," in *Proc. ICC '99*, Vancouver, Canada, 1999, pp. 231–235.

[19] S. B. Weinstein and P. M. Ebert, "Data transmission by frequency-division multiplexing using the discrete Fourier transform," *IEEE Trans. Commun. Technol.*, vol. CT-19, pp. 626–634, Oct. 1971.

[20] J. A. C. Bingham, "The DSL as a medium for high-speed data," in *Multicarrier Modulation and xDSL*. New York: Wiley, 2000, ch. 3.

[21] N. Al-Dhahir, "FIR channel-shortening equalizers for MIMO ISI channels," *IEEE Trans. Commun.*, vol. 49, pp. 213–218, Feb. 2001.

[22] K. W. Cheong and J. M. Cioffi, "Precoder for DMT with insufficient cyclic prefix," in *Proc. ICC '98*, Atlanta, GA, 1998, pp. 339–343.

[23] G. Ginis and J. M. Cioffi, "A multi-user precoding scheme achieving crosstalk cancellation with applications to DSL systems," in *Proc. 34th Asilomar Conf. Signals, Systems, and Computers*, Pacific Grove, CA, Oct. 2000, pp. 1627–1631.

[24] M. Tomlinson, "New automatic equaliser employing modulo arithmetic," *Electron. Lett.*, vol. 7, pp. 138–139, Mar. 1971.

[25] H. Harashima and H. Miyakawa, "Matched-transmission technique for channels with intersymbol interference," *IEEE Trans. Commun.*, vol. COM-20, pp. 774–780, Aug. 1972.

[26] G. Ginis and J. M. Cioffi, "Vectored-DMT: A FEXT canceling modulation scheme for coordinating users," in *Proc. ICC 2001*, vol. 1, Helsinki, Finland, June 2001, pp. 305–309.

[27] J. M. Cioffi and G. D. Forney, "Generalized decision-feedback equalization for packet transmission with ISI and Gaussian noise," in *Communication, Computation, Control and Signal Processing (A tribute to Thomas Kailath*, A. Paulraj, V. Roychowdhury, and C. Schaper, Eds. Boston, MA: Kluwer, 1997, ch. 4, pp. 79–127.

[28] P. W. Wolniansky, G. J. Foschini, G. D. Golden, and R. A. Valenzuela, "V-BLAST: An architecture for realizing very high data rates over the rich-scattering wireless channel," in *Proc. URSI ISSSE '98*, Pisa, Italy, pp. 295–300.

[29] G. J Foschini, G. D Golden, R. A. Valenzuela, and P. W. Wolniansky, "Simplified processing for high spectral efficiency wireless communication employing multielement arrays," *IEEE J. Select. Areas Commun.*, vol. 17, pp. 1841–1852, Nov. 1999.

[30] G. Ginis and J. M. Cioffi, "On the relation between V-BLAST and the GDFE," *IEEE Commun. Lett.*, vol. 5, pp. 364–366, Sept. 2001.

[31] S. Verdu, *Multiuser Detection*. Cambridge, MA: Cambridge Univ. Press, 1998.

[32] G. H. Golub and C. F. Van Loan, "Orthogonalization and least squares," in *Matrix Computations*, 3rd ed. Baltimore, MD: Johns Hopkins Univ. Press, 1996, ch. 5.

[33] J. M. Cioffi. Course notes for EE379A—Digital communication. Stanford Univ., Stanford, CA. [Online]. Available: http://www.stanford.edu/class/ee379a/reader.html.

[34] K. S. Jacobsen, "Methods of upstream power backoff on very high-speed digital subscriber lines," *IEEE Commun. Mag.*, pp. 210–216, Mar. 2001.

[35] W. Yu, G. Ginis, and J. M. Cioffi, "An adaptive multiuser power control algorithm for VDSL," *IEEE J. Select. Areas Commun.*, vol. 20, June 2002.

[36] C. Zeng, Carlos Aldana, Atul Salvekar, and J. M. Cioffi, "Crosstalk identification in xDSL systems," *IEEE J. Select. Areas Commun.*, vol. 19, pp. 1488–1496, Aug. 2001.

[37] J. M. Cioffi. (2001, Feb.) Proposal for study of dynamic spectrum management for the evolving unbundling architecture of DSL. T1E1.4 Contribution 2001-090, Los Angeles, CA. [Online]. Available: http://www.t1.org/

[38] C. Y. Wong, R. Cheng, K. B. Letaief, and R. D. Murch, "Multiuser OFDM with adaptive subcarrier, bit, and power allocation," *IEEE J. Select. Areas Commun.*, vol. 17, pp. 1747–1758, Oct. 1999.

[39] W. Yu and J. M. Cioffi, "FDMA capacity of the Gaussian multiple access channel with ISI," in *Proc. ICC 2000*, New Orleans, LA, pp. 1365–1369.

[40] V. Oksman and J. M. Cioffi. (1999, December) Noise models for VDSL performance verification. T1E1.4 Contribution 99-438R2, Clearwater, FL. [Online]. Available: http://www.t1.org/.

[41] A. Leke and J. M. Cioffi, "Impact of imperfect channel knowledge on the performance of multicarrier systems," in *Proc. Globecom'98*, Sydney, Australia, pp. 951–955.

[42] K. S. Jacobsen. (1998, Nov.) The equalized-FEXT upstream power cutback method to mitigate the near–far problem in VDSL. ETSI TM6 Contribution TD05, Sophia Antipolis, France. [Online]. Available: http://www.etsi.org/

[43] Stanford Business Software Inc, Stanford, CA. SOL optimization software. [Online]. Available: http://www.sbsi-sol-optimize.com/index.html

[44] J. Cook. (2000, Feb.) Proposed VDSL band plans. ETSI TM6 Contribution TD13, Montreux, Switzerland. [Online]. Available: http://www.etsi.org/

[45] S. Kasturia, J. Aslanis, and J. M. Cioffi, "Vector coding for partial-response channels," *IEEE Trans. Inform. Theory*, vol. 36, pp. 741–762, July 1990.
[46] R. G. Gallager, "Energy limited channels: Coding, multiaccess and spread spectrum," in *Proc. Conf. Inform. Sci. Syst.*, Mar. 1988, p. 372.
[47] W. Yu, W. Rhee, S. Boyd, and J. M. Cioffi, "Iterative waterfilling for Gaussian vector multiple access channels," in *Proc. Int. Symp. Inform. Theory 2001*, Washington, DC, June 2001, p. 322.
[48] G. Caire and S. Shamai, "On achievable rates in a multi-access Gaussian broadcast channel," in *Proc. Int. Symp. Inform. Theory 2001*, Washington, DC, June 2001, p. 147.
[49] U. Erez, S. Shamai, and R. Zamir, "Capacity and lattice-strategies for cancelling known interference," in *Proc. Int. Symp. Information Theory and Applications*, Honolulu, HI, Nov. 2000, pp. 681–684.
[50] W. Yu and J. M. Cioffi, "Sum capacity of Gaussian vector broadcast channels," presented at the Int. Symp. Inform. Theory 2002, Lausanne, Switzerland, July 2002.
[51] S. Boyd and L. Vandenberghe. Course notes for EE364—Convex optimization. Stanford University, Stanford, CA. [Online]. Available: http://www.stanford.edu/class/ee364/

George Ginis (S'97) received the Diploma in electrical and computer engineering from the National Technical University of Athens, Athens, Greece, in 1997, and the M.S. and Ph.D. degrees in electrical engineering from Stanford University, Stanford, CA, in 1998 and 2002, respectively. He is currently with the Broadband Communications Group of TI, San Jose, CA.

His research interests include multiuser transmission theory, interference mitigation, and their applications to wireline and wireless communications.

John M. Cioffi (S'77–M'78–SM'90–F'96) received the B.S.E.E degree from the University of Illinois, Urbana-Champaign, in 1978 and the Ph.D.E.E. degree from Stanford University, Stanford, CA, in 1984.

He was with Bell Laboratories, Holmdel, NJ, from 1978 to 1984 and IBM Research, San Jose, CA from 1984 to 1986. He has been with Stanford University as an Electrical Engineering Professor from 1986 to the present. He founded Amati Communications Corporation, Palo Alto, CA, in 1991 (it was purchased by Texas Instruments, Incorporated in 1997), and was Officer/Director from 1991 to 1997. He is currently on the boards or advisory boards of BigBand Networks, Coppercom, GoDigital, Ikanos, Iospan, Ishoni, IteX, Marvell, Kestrel, Charter Ventures and Portview Ventures. He is a Member of the U.S. National Research Council's CSTB. His specific interests are in the area of high-performance digital transmission.

Dr. Cioffi has received the following awards: the National Academy of Engineering in 2001, IEEE Kobayashi Medal in 2001, IEEE Millennium Medal in 2000, IEE JJ Tomson Medal in 2000, 1999 University of Illinois Outstanding Alumnus, 1991 IEEE COMMUNICATIONS MAGAZINE best paper; 1995 ANSI T1 Outstanding Achievement Award, and NSF Presidential Investigator from 1987 to 1992. He became a member of the National Academy of Engineering in 2001. He has published over 200 papers and holds over 40 patents, most of which are widely licensed, including basic patents on DMT, VDSL, and V-OFDM.